Engineered Extracellular Vesicles Enriched with miR-214 Enhance the Efficacy of Chemotherapy for Ovarian Cancer

Weida Wang[#, 1], Ayesha Alvero[#, 2], Yi Qin[1], Mingjin Wang[1], Alexandra Fox[2], Yanfeng Li[1], Michael Millman[1], Amy Kemper[3], Gil Mor[2], Xian Shuang Liu[1], Michael Chopp[1,4], Zheng Gang Zhang[*, 1] and Yi Zhang[*, 1]

1 Department of Neurology, Henry Ford Hospital, Detroit, MI, United States.

2 C.S. Mott Center for Human Growth and Development, Department of Obstetrics and Gynecology, Wayne State University, Detroit, MI, United States.

3 Department of Pathology, Henry Ford Hospital, Detroit, MI, United States.

4 Department of Physics, Oakland University, Rochester, MI, United States.

Co-first authors, Weida Wang and Ayesha Alvero, contribute equally to this manuscript.

*, Corresponding authors

Zheng Gang Zhang, zzhang1@hfhs.org

Yi Zhang, yzhang3@hfhs.org

Acknowledgements:

We thank Dr. Paul Stemmer from Wayne State University Proteomics Core for mass spectrometry-based proteomics. The Proteomics Core is supported, in part, by NIH Center grant P30 CA022453 to the Karmanos Cancer Institute at Wayne State University.

Funding:

This work was supported by the NIH grant R01 CA219829-01A1 (ZGZ) and the Janet Burros Memorial Foundation (AA).

Abstract

Recurrent ovarian cancer (OC) remains a major cause of mortality due to chemoresistance and metastasis. Epigenetic dysfunction, particularly involving microRNAs (miRNAs), contributes to disease progression. Extracellular vesicles (EVs) are key modulators of tumor epigenetic profiles by delivering bioactive cargo to recipient cells. Here, we demonstrate that engineered small EVs derived from cerebral endothelial cells and enriched with miR-214-3p (m214-sEVs) enhance chemosensitivity, suppress tumor growth, and improve survival when combined with carboplatin. Using a clinically relevant mouse model that mimics spontaneous OC relapse following first-line platinum-based chemotherapy, we showed that m214-sEVs were internalized by OC cells and the OC niche fibroblasts via clathrin-mediated endocytosis, resulting in the elevation of miR-214-3p/miR-199a-5p and the downregulation of chemoresistance-associated genes, including toll-like receptor 4 (TLR4), β-catenin, and the soluble N-ethylmaleimide-sensitive factor attachment protein receptor (SNARE) protein YKT6. Moreover, secondary tumor-derived sEVs (t-sEVs) released by OC and niche cells that internalized m214-sEVs reduced pro-metastatic proteins, such as integrin β1 and matrix metalloproteinase 9 (MMP9), in their cargo and limited their capacity to promote invasion and resistance. In vitro, YKT6 overexpression in ovarian cancer stem cells (OCSCs) attenuated the effect of m214-sEVs on sensitizing carboplatin to block OCSC migration. These findings support the translational potential of miRNA-loaded sEVs (m214-sEVs) as a therapeutic strategy to overcome chemoresistance and recurrence in OC.

Introduction

Ovarian cancer (OC) is a highly heterogeneous disease characterized by diverse cellular phenotypes that drive its complexity and contribute to its high recurrence rate[1-4]. Recurrent OC remains largely incurable due to the development of acquired resistance to standard therapies and aggressive metastatic behavior, with second-line treatments rarely yielding durable responses[5,6]. Compared to primary tumors, recurrent OC is enriched in ovarian cancer stem cells (OCSCs) and cancer-associated stromal cells, such as fibroblasts, populations known for their plasticity and role in promoting therapeutic resistance and poor clinical outcomes[7-12].

MicroRNA (miRNA) dysregulation is a hallmark of epigenetic dysfunction in cancer and plays a critical role in regulating gene networks that drive OC progression and influence treatment response[13-16]. In OC, miRNA dysfunction contributes to tumor heterogeneity and often exhibits complex, cell-type–specific effects[17-19]. This regulatory complexity is further shaped by interactions among diverse cell populations within the tumor microenvironment. While specific oncogenic miRNAs enhance tumor aggressiveness, the loss of tumor-suppressive miRNAs is frequently associated with poor prognosis[20,21]. Clinically, although some studies report miR-214 upregulation[22,23], approximately 45% of patients with advanced-stage OC and 60% of those with high-grade serous ovarian carcinoma (HGSOC) exhibit significant downregulation of miR-214, which correlates with reduced survival[23,24]. Functionally, miR-214 overexpression has been shown to inhibit OC growth by suppressing phosphatase and tensin homolog deleted on chromosome 10 (PTEN) and semaphorin signaling[22,25]. Our previous work demonstrated that loss of the miR-214-3p/199a-5p cluster in OCSCs promotes tumor progression and chemoresistance[26,27]. Collectively, these findings support a role for miR-214 as a context- and cell-type–specific tumor suppressor in OC.

Small extracellular vesicles (sEVs) are membrane-bound nanovesicles secreted by nearly all cell types and serve as key mediators of intercellular communication through the transfer of bioactive cargo, including miRNAs[28-32]. Compared to synthetic delivery systems, sEVs offer superior delivery efficiency and retain molecular signatures from their cells of origin, facilitating targeted, cell-specific interactions [33-36] . Within the tumor microenvironment, sEVs are potent modulators of epigenetic regulation, influencing critical processes such as chemoresistance, metastasis, and therapeutic response[14,37,38]. While tumor-derived sEVs often promote tumor growth, immune evasion, and drug resistance[39,40], sEVs released from non-malignant cells, such as mesenchymal stromal cells (MSCs)[41,42], fibroblasts[43], and cerebral endothelial cells (CECs)[18,44], can exhibit tumor-suppressive functions.

In our previous work, CEC-derived sEVs (CEC-sEVs) were shown to mitigate chemotherapy-induced peripheral neuropathy and enhance the cytotoxic response of OC cells. These effects were partly mediated by downregulating miR-214-3p targets implicated in neurotoxicity and tumor progression[18]. Building on these findings, the present study employs a clinically relevant mouse model of recurrent OC to test the hypothesis that engineered CEC-sEVs enriched with miR-214-3p (m214-sEVs) enhance the efficacy of chemotherapy.

Results

Chemoresistant Recurrent OC is Characterized by Low Levels of miR-214-3p and miR-199a-5p

We first generated a xenograft model of recurrent OC by treating mice bearing OVCAR3/luc [18] with carboplatin at a clinically comparable regimen (60 mg/kg, administered via tail vein on days 7 (week 1; W1) and 14 (week 2; W2) post-implantation) [45,46] (**Fig.1A**). Six weeks (W6) after the final dose of carboplatin, bioluminescence imaging (BLI) showed tumor signals at background levels, with total flux < 5×10□ p/s/cm² (**Fig.1A**). However, approximately 40% of mice developed recurrent tumors (total flux > 1×10□ p/s/cm²) as early as eight weeks post-treatment (referred to here as recurrent week 0 (RW0), **Fig. 1A**). The recurrent tumors exhibited aggressive growth, leading to 100% mortality within eight weeks after recurrence (RW8, **Fig. 1A**). This is consistent with our previous findings showing OC relapse following chemotherapy in mice bearing OCSC xenografts[9].

We previously identified miR-214-3p and its cluster partner miR-199a-5p as among the most significantly downregulated miRNAs in chemoresistant OCSCs compared to chemosensitive counterparts[26]. Consistent with this finding, we compared primary and recurrent OVCAR3/luc tumors and observed significantly reduced levels of miR-214-3p and miR-199a-5p in the recurrent/chemoresistant tumors relative to primary OC xenografts (**Fig. 1B**). Moreover, in situ hybridization (ISH) analysis of tumor specimens from patients with recurrent HGSOC revealed that miR-214-3p and miR-199a-5p were undetectable in tumor cells, however, it showed strong expression in adjacent stromal cells (**Supplemental Fig. 1**). Together, these findings demonstrate that miR-214-3p and miR-199a-5p are differentially expressed within the tumor microenvironment in recurrent chemoresistant xenografts and human OC tissues, suggestive of their role as tumor-suppressive miRNAs in advanced and recurrent OC

Engineered miR-214-3p-enriched sEVs Enhance Treatment Efficacy of Recurrent OC with Carboplatin

To investigate whether engineered sEVs enriched with miR-214-3p enhance chemotherapy response in recurrent OC, we generated CEC-sEVs enriched with miR-214-3p (m214-sEVs) by isolating sEVs from conditioned media of human healthy CECs transfected with a lentiviral vector encoding miR-214-3p (m214-CECs). As control, we used a vector carrying a scramble

sequence (scra-CECs), as previously described[47]. Following the Minimal Information for Studies of Extracellular Vesicles (MISEV) 2018 and 2023 guidelines[48,49], we performed a series of characterization assays. Transmission electron microscopy (TEM), cryo-electron microscopy, and nanoparticle tracking analysis (NTA) showed that m214-sEVs and sEVs from scramble-transfected CECs (scra-sEVs) exhibited comparable sEV-specific morphology and membrane-enclosed structures, with no significant differences in particle size or concentration (**Fig. 2A-D**). Western blot and Exoview analyses confirmed that transmembrane tetraspanin proteins (CD63, CD81, CD9) among the naïve CEC-sEVs, scra-sEVs, and m214-sEVs were comparable, while endoplasmic reticulum (ER) membrane protein was absent (**Fig. 2E-F**, **Supplemental Fig. 2**). Collectively, these data show that the miR-214 transfection does not affect sEV morphology or yield.

To assess cargo composition, qRT-PCR was performed and revealed that m214-sEVs contained approximately an 11-fold increase and a 6-fold increase in miR-214-3p and miR-199a-5p, respectively, compared to scra-sEVs and naïve CEC-sEVs (**Fig. 2G**). Notably, levels of unrelated miRNAs (miR-15b-5p, miR-16-2) remained unchanged, indicating selective enrichment of the miR-214-3p/miR-199a-5p cluster. Proteomic analysis showed that the overall protein composition of m214-sEVs was comparable to that of naïve CEC-sEVs (**Supplemental Excel 1**). The most enriched Gene Ontology (GO) terms included cadherin binding and RNA binding processes, which are functions associated with sEV–recipient cell interactions and cargo sorting, respectively (**Supplemental Fig. 3, Supplemental Excel 2**). These results confirm that m214-sEVs selectively enrich therapeutic miRNAs without altering the core protein cargo.

To evaluate the therapeutic efficacy of m214-sEVs *in vivo*, we utilized the OVCAR3/luc recurrent xenograft model described above. Mice were treated with carboplatin at W1 and W2 post–cancer cell injection, as shown in **Fig. 1A**, and then monitored for tumor recurrence. Upon recurrence (RW1 timepoint), animals were randomized into four treatment groups: (1) PBS control, (2) carboplatin monotherapy, (3) combination therapy with carboplatin and scra-sEVs, and (4) combination therapy with carboplatin and m214-sEVs (**Fig. 3A**). Carboplatin (60mg/kg) was administered at RW1 and RW2, while sEVs (1×10^{11} particles/injection) were delivered intraperitoneally (i.p.) every other day for six consecutive weeks (**Fig. 3A**). Control animals received PBS on the same schedule.

The PBS-treated group exhibited rapid tumor progression, with all animals reaching experimental endpoint by RW6 (**Fig. 3B–D**). Treatment with carboplatin alone or in combination

with scra-sEVs significantly decreased tumor growth compared to PBS control, but still, all animals in these groups reached the endpoint by RW10 (**Fig. 3B–D**). Strikingly, mice treated with the combination of carboplatin and m214-sEVs showed disease regression with tumor burden significantly less than the other treated groups by the RW1 timepoint (**Fig. 3B, C**). More importantly, the combination of carboplatin and m214-sEVs significantly improved overall survival, with all animals surviving beyond 200 days post-recurrence (**Fig. 3D**). These results demonstrate that m214-sEVs significantly enhance the efficacy of carboplatin,_providing sustained therapeutic benefit.

m214-sEVs Enable Chemotherapy Dose Reduction While Maintaining Efficacy in Primary OC

Although carboplatin-based chemotherapy is effective for treating primary OC, its dose-dependent toxicities limit long-term use[50,51]. Building on our previous findings that m214-sEVs enhance the efficacy of carboplatin in recurrent OC, we next investigated whether combining m214-sEVs with a reduced dose of carboplatin could effectively suppress the progression of primary OC tumors. Thus, mice bearing primary OVCAR3/luc xenografts were treated at W1 and W2 as in **Fig. 1A** with a reduced dose of carboplatin (30 mg/kg, i.v.). This dose represents a 50% reduction compared to the dose used in the recurrent OC model shown in **Fig. 3**. Concurrently, starting from the first dose of carboplatin, mice received i.p. injections of m214-sEVs or scra-sEVs (1×10^{11} particles/injection) every other day for six consecutive weeks (**Fig. 4A**).

Consistent with our and others' previous findings[18,52,53], primary OC xenografts responded to carboplatin monotherapy, and the addition of scra-sEVs further suppressed tumor growth by 46% (W6) compared to carboplatin alone (**Fig. 4B-D**). Importantly, the combination of m214-sEVs with low-dose carboplatin resulted in a significantly greater suppression of tumor growth, an addition of 45% (W6) compared to the combination of carboplatin and scra-sEVs (**Fig. 4B-D**). These results demonstrate that m214-sEVs can markedly enhance the antitumor efficacy of carboplatin in primary OC models, enabling a reduction in chemotherapy dose while achieving superior therapeutic outcomes.

m214-sEVs Sensitize Chemoresistant OC Cells to Platinum and Taxane Therapies *in vitro*

As advanced HGSOC frequently develops resistance to frontline chemotherapy[54,55], we further

investigated whether m214-sEVs can sensitize additional chemoresistant OC models to platinum- or taxane-based treatments. Cisplatin-resistant A2780cis cells were treated with cisplatin in combination with sEVs at concentrations of 3×10□, 3×10□, and 3×10□ particles/mL. Neither scra-sEV nor naïve CEC-sEV significantly altered cisplatin IC_{50} values, indicating no enhancement of cisplatin-induced cytotoxicity. In contrast, m214-sEVs significantly reduced IC_{50} values at all tested concentrations, demonstrating potent chemosensitization of A2780cis cells (**Fig. 5A**). Notably, 3×10□ particles/mL of m214-sEVs achieved comparable sensitization to the higher 3×10□ dose, establishing 3×10□ particles/mL as the optimal concentration for subsequent *in vitro* experiments.

We next examined the effect of m214-sEVs on patient-derived paclitaxel-resistant OCSCs (OCSC-R182 and OCSC-R2615)[8,9,56]. CellTox Green cytotoxicity assays demonstrated that m214-sEVs, but not scra-sEVs, significantly enhanced paclitaxel (20 μM)-induced cell death compared to paclitaxel alone. Neither m214-sEVs nor scra-sEVs alone had a significant effect on viability (**Fig. 5B, Supplemental Fig. 4**). These findings collectively demonstrate that m214-sEVs can directly sensitize chemoresistant ovarian cancer cells, including patient-derived OCSCs, to platinum and taxane chemotherapy, supporting their potential as a therapeutic adjunct for treatment-resistant OC.

m214-sEVs Elevate miR-214-3p/miR-199a-5p and Reduce TLR4 and β-catenin in OC

To investigate the mechanisms underlying the ability of m214-sEVs to sensitize OC to chemotherapy, we assessed whether exogenously administered m214-sEVs are internalized by OC tumors *in vivo*. Thus, mice bearing recurrent OC were injected i.p. with GFP-labeled m214-sEVs (GFP-m214-sEVs). Control mice were administered unlabeled m214-sEVs (**Fig. 6A**). Confocal microscopy revealed GFP-positive signals within OC tumors from mice injected with GFP-m214-sEVs. GFP signal was not detectable in tumors from mice treated with unlabeled m214-sEVs, confirming the specificity of the GFP signal (**Fig. 6B**). Immunogold electron microscopy further showed GFP-positive gold particles within both OC cells and adjacent fibroblasts, indicating uptake by both tumor and stromal cells (**Fig. 6C-E**).

In mice bearing mCherry-labeled OCSC1-F2 tumors, we further examined the biodistribution of m214-sEVs following administration using Gaussia luciferase–labeled m214-sEVs (Gluc-m214-sEVs) (**Fig. 6F**), which offer high sensitivity for luminescence-based detection[57]. Combined BLI and fluorescence imaging revealed that i.p. administered Gluc-m214-sEVs selectively

accumulated in mCherry-positive tumor nodules, with minimal signal detected in major intraperitoneal organs (**Fig. 6G**).

To examine the uptake mechanism, we pretreated paclitaxel-resistant OCSC-R182 cells *in vitro* with chlorpromazine (CPZ), an inhibitor of clathrin-mediated endocytosis[29,58]. CPZ pretreatment abolished the ability of m214-sEVs to enhance paclitaxel-induced cell death, indicating that clathrin-dependent endocytosis is required for sEV internalization and function (**Fig. 6H**). Together, these results show that m214-sEVs are internalized by OC tumors and that this is required for their function.

We next investigated whether m214-sEVs modulate miR-214-3p and miR-199a-5p levels in recurrent OC tumors. qRT-PCR analysis of recurrent intraperitoneal tumors collected at the RW4 time-point (**Fig. 7A**) showed that the combination therapy of carboplatin and m214-sEVs significantly increased the levels of both miR-214-3p and miR-199a-5p compared to carboplatin monotherapy or the combination therapy of carboplatin and scra-sEVs (**Fig. 7B**). Fluorescent in situ hybridization (FISH) further showed that carboplatin alone or in combination with scra-sEV reduced miR-214-3p expression (**Fig. 7C**). These findings demonstrate that m214-sEVs restore and elevate chemotherapy-suppressed miR-214-3p/miR-199a-5p expression in the tumor microenvironment.

Toll-like receptor 4 (TLR4) and β-catenin, two validated direct target genes of miR-214-3p[59,60], are critical mediators of chemoresistance and metastasis in OC[26,27,61]. Our previous studies demonstrated that miR-199a-5p regulates chemoresistance through the TLR4 pathway[26] and that β-catenin is selectively upregulated in chemoresistant OCSCs[61]. Western blot analysis of recurrent OC tumors showed that carboplatin monotherapy significantly increased TLR4 and β-catenin, consistent with their established roles in acquired chemoresistance[62,63]. In contrast, the combination treatment with carboplatin and m214-sEVs markedly reduced the expression of both proteins. Importantly, this combination also elevated levels of cleaved (active) caspase-3, indicating enhanced apoptosis in chemoresistant OC tumors (**Fig. 8C–D**).

In vitro, m214-sEVs combined with paclitaxel also significantly reduced paclitaxel-induced upregulation of TLR4 and β-catenin in OCSC-R182 cells (**Fig. 8E–F**) and significantly increased caspase-3/7 activity, suggesting potentiated apoptotic response (**Fig. 8G**). In contrast, scra-sEVs, either alone or combined with chemotherapy, did not affect TLR4 or β-catenin expression and did not enhance apoptosis (**Fig. 8E–F**).

To further determine the functional contribution of sEV cargo, we conducted an EV cargo protection assay by treating m214-sEVs with proteinase K or RNase, in the presence or absence of the membrane-disrupting detergent Triton X-100[64]. Treatment with proteinase K or RNase in the presence of Triton X-100 abolished the cytotoxic effect of m214-sEVs (**Supplemental Fig. 5**). In contrast, treatment with either enzyme in the absence of Triton X-100 preserved their cytotoxic activity (**Supplemental Fig. 5**). These findings indicate that the therapeutic effect of m214-sEVs is mediated primarily by the sEV encapsulated molecules, such as miRNAs, rather than surface-bound proteins or RNAs.

Together, these findings suggest that m214-sEVs modulate the levels of miR-214-3p/miR-199a-5p and the downregulation of their known targets TLR4 and β-catenin in recurrent OC tumors. These molecular changes are accompanied by enhanced sensitivity of chemoresistant OC cells to carboplatin and paclitaxel and increased apoptosis, indicating a potential link between miRNA modulation and therapeutic response.

m214-sEV and Carboplatin Combination Therapy Alters Secondary Tumor-Derived sEVs Toward a Less Pro-tumorigenic Phenotype in Recurrent OC

Further ultrastructural analysis of immunogold-labeled OC tumors from mice treated with GFP-labeled m214-sEVs in combination with carboplatin revealed abundant GFP-positive signals within intraluminal vesicles of multivesicular bodies (MVBs) in OC cells (**Fig. 9B**). These findings indicate the presence of internalized m214-sEVs within the MVB compartment, suggesting that m214-sEVs could be recycled. Furthermore, GFP signals were also detected on vesicular structures in the adjacent extracellular space (**Fig. 9C**), suggesting that m214-sEVs could interact with tumor niche cells. Primary tumor cell–derived sEVs (t-sEVs) are known to promote cancer cell survival, chemoresistance, and metastasis[65-67]; however, emerging evidence[68,69], including the concept proposed by Askenase[70], suggests that secondary EVs released by the tumor and its niche cells that take up exogenous EVs may possess distinct properties and biological functions from primary t-sEVs. We thus hypothesized that secondary t-sEVs produced by m214-sEV recipient tumor and its niche cells in the recurrent OC mouse shift from a pro-tumorigenic to a less tumor-promoting, or a potentially anti-tumorigenic, phenotype. To test this, we harvested tumor tissues from recurrent OC-bearing mice four weeks after the initiation of the combination treatment, and cultured them *ex vivo* for 24 hours to collect secondary t-sEVs (**Fig. 9D**). Using these t-sEVs (3×10□ particles/mL), we then treated mCherry-labeled chemoresistant

OCSC1-F2 cells[9]. Secondary t-sEVs from PBS- or carboplatin-only–treated mice (PBS-t-sEVs and carbo-t-sEVs) significantly increased the IC_{50} of carboplatin, suggesting that these t-sEVs promote chemoresistance. In contrast, t-sEVs isolated from mice that received the combination treatment (m214 + carbo-t-sEVs) significantly reduced the cisplatin IC_{50}, indicating a loss of their pro-resistance function (**Fig. 9E**). We further analyzed the protein cargo of these secondary t-sEVs. Western blot analysis revealed that Carbo-t-sEVs contained elevated levels of integrin β1 and matrix metalloproteinase-9 (MMP9), both of which are associated with extracellular matrix remodeling, stemness, invasion, and chemoresistance[71-73]. In contrast, m214+Carbo-t-sEVs showed significantly reduced levels of integrin β1 and MMP9 compared to both PBS-t-sEVs and Carbo-t-sEVs (**Fig. 9F–G**). Interestingly, MMP2 levels remained unchanged across all treatment groups. Consistent with the protein data, invasion assays showed that PBS-t-sEVs and Carbo-t-sEVs enhanced the invasive capacity of OCSC-F2 cells, whereas m214+Carbo-t-sEVs had no such effect, indicating a loss of pro-metastatic potential (**Fig. 9H**). Together, these findings indicate that m214-sEV–based combination therapy is associated with the release of secondary t-sEVs with diminished pro-tumorigenic properties, which together with m214-sEVs could contribute to enhanced effect of chemotherapy on the suppression of recurrent OC.

YKT6 Overexpression Abrogates the Anti-Migratory and sEV-Modulating Effects of m214-sEV plus Carboplatin Treatment

We found that treatment with m214-sEVs combined with carboplatin significantly reduced the expression of YKT6, one of the predicted target genes of miR-214-3p, in recurrent OC tissues (**Fig. 10BC**). Consistently, proteomic profiling of OVCAR3 cells treated with m214-sEVs revealed a downregulation of YKT6 (**Supplemental Excel 1**). YKT6 is a member of the vesicular soluble N-ethylmaleimide-sensitive factor attachment protein receptor (v-SNARE) family [74,75], and promotes metastasis in lung and breast cancers by driving epithelial–mesenchymal transition (EMT) and enhancing matrix metalloproteinase (MMP) activity[76-78].

To investigate whether YKT6 contributes to the therapeutic effects of the combination treatment in recurrent OC, we performed a gain-of-function study by generating a YKT6-overexpressing OCSC1-F2 cell line (YKT6-F2) using retroviral transduction (Addgene #116946, pMRXIP-GFP-YKT6). Western blot analysis confirmed successful YKT6 overexpression in YKT6-F2 cells compared to control vector-transduced F2 cells (vector-F2) (**Supplemental Fig. 6 A, B**).

Migration assays showed that treatment of vector-F2 cells with the combination of m214-sEVs and carboplatin significantly suppressed cell migration compared to either scra-sEVs plus carboplatin or carboplatin alone (**Fig. 10D**). In contrast, this combination treatment did not reduce the migration of YKT6-F2 cells, indicating that YKT6 overexpression abrogates the anti-migratory effect (**Fig. 10D**). Notably, no significant differences in migration were observed between vector-F2 and YKT6-F2 cells under PBS, monotherapies (carboplatin, scra-sEVs, m214-sEVs), or the scra-sEV plus carboplatin treatment (**Fig. 10D**). These findings suggest that the inhibitory effect of m214-sEV and carboplatin combination treatment on F2 cell migration is specific and YKT6-dependent. Together, these *in vitro* results support a role for YKT6 downregulation in mediating the therapeutic activity of m214–sEV–based combination treatment of recurrent OC.

Given YKT6's established role in EV biogenesis and cargo loading[79-82] , we next examined whether YKT6 overexpression influences tumor-derived sEV (t-sEV) production and content. NTA and TEM results revealed no significant differences in particle concentration or morphology between YKT6-F2, vector-F2, and parental OCSC1-F2 cells (**Fig. 10E–G, Supplemental Fig. 6C**). However, sEVs from YKT6-F2 cells (YKT6-t-sEVs) exhibited significantly increased particle size (**Fig. 10F**) and were enriched with pro-metastatic proteins, including integrin β1, MMP2, and MMP9, compared to control vector-derived sEVs (**Fig. 10H–I**). These *in vitro* findings, together with the observed *in vivo* downregulation of YKT6 by the m214-sEV and carboplatin combination therapy, support a model in which YKT6 suppression contributes to the therapeutic efficacy of the combination treatment by limiting the production of pro-tumorigenic t-sEVs in recurrent OC.

..

Discussion

Recurrent OC remains incurable, primarily due to the development of chemoresistance and metastatic progression[83,84]. In this study, we demonstrate that engineered m214-sEVs, enriched with miR-214-3p and miR-199a-5p, enhance chemosensitivity and suppress tumor growth in models of recurrent OC. These therapeutic effects appear to be mediated via the downregulation of chemoresistance-associated genes such as TLR4 and β-catenin (**Fig. 11A**), as well as by inhibition of the SNARE protein YKT6 (**Fig. 11B**). Our findings also suggest that secondary tumor-derived sEVs generated by tumor and niche cells in response to m214-sEV and carboplatin treatment possess reduced pro-tumorigenic activity, suggesting that secondary tEVs together with m214-sEVs contribute to the efficacy of combination therapy on suppression of disease recurrence.

We employed a clinically relevant OC mouse model that recapitulates relapse following first-line platinum-based chemotherapy. Unlike models that rely on prolonged drug exposure or artificial induction of resistance[85-87], this model enables spontaneous OC recurrence, capturing the complexity of intratumoral heterogeneity, including OCSCs, stromal fibroblasts, and immune cell populations[9,88-90]. Importantly, this model also reflects the miRNA heterogeneity seen in OC tumors. In situ hybridization revealed consistent downregulation of the miR-214-3p/miR-199a-5p cluster in recurrent OC tumors and human HGSOC, while adjacent stromal cells retained expression of this cluster, indicating a cell–type–specific pattern. Treatment with m214-sEVs in combination with carboplatin resulted in sustained tumor suppression for more than 200 days, whereas monotherapies led to tumor recurrence. In vitro, m214-sEVs enhanced chemosensitivity across multiple chemoresistant and recurrent OC cell lines. Moreover, internalization of m214-sEVs by tumor cells increased intracellular levels of the miR-214-3p/199a-5p cluster. Together, these findings highlight the therapeutic potential of this miRNA cluster in overcoming chemoresistance in recurrent OC.

sEVs are increasingly recognized as promising therapeutic vehicles due to their biocompatibility and ability to deliver functional cargo to recipient cells[33-36]. However, the intracellular mechanisms by which EV cargo exerts its effects on recipient cells remain incompletely understood. In this study, m214-sEVs suppressed the expression of known miR-214-3p/miR-199a-5p target genes—TLR4, β-catenin, and YKT6, which are key regulators of tumor progression, metastasis, and chemoresistance[26,27,61,76-78]. A gain-of-function experiment revealed that YKT6 overexpression in OCSCs abrogated the anti-migratory effects of the m214-sEV and carboplatin combination treatment, implicating YKT6 as a critical functional target of

the therapy. Furthermore, m214-sEVs were taken up by adjacent stromal fibroblasts, indicating that the combination treatment may also modulate the tumor microenvironment by influencing non-malignant niche cells.

Compared to primary tumor-derived sEVs (t-sEVs), the role of secondary t-sEVs in modulating tumor progression remains understudied[70]. The present study showed that secondary tEVs generated by tumor and its niche cells that internalized m214-sEVs in response to the combination treatment with m214-sEVs and carboplatin changed primary t-sEVs from a pro-tumorigenic to an anti-tumorigenic state, as evidenced by a marked reduction in cargo proteins such as integrin β1 and MMP9. Consistent with the known role of YKT6 in regulating EV cargo sorting through endosomal membrane cycling[79-82], our data suggest that YKT6 plays a key role in determining the protein composition of t-sEVs. Specifically, t-sEVs derived from YKT6-overexpressing OCSCs were enriched in pro-metastatic proteins and were able to override the anti-migratory effects of m214-sEV and carboplatin combination treatment. These findings indicate that the therapeutic benefit of the combination therapy extends beyond direct effects on tumor cells to include modulation of secondary t-sEV cargo content. This supports the emerging concept proposed by Askenase[70] that secondary EVs, in concert with m214-sEVs, collectively shape the biological outcome of the combination intervention.

Given that secondary EV-mediated signaling plays a critical role in regulating immune cell responses, particularly macrophage polarization[68-70] , we speculate that the therapeutic efficacy of m214-sEVs in combination with carboplatin may, in part, be driven by immunomodulatory mechanisms. This potential effect on the immune compartment warrants further investigation to fully elucidate the role of EV-mediated crosstalk in the anti-tumor activity of the combination therapy.

Together, these findings provide compelling evidence that m214-sEVs, when combined with carboplatin, offer a promising strategy to overcome chemoresistance and suppress recurrence in OC. By delivering tumor-suppressive miRNAs and modulating both tumor-intrinsic pathways and the composition of secondary tumor-derived sEVs, this combination therapy targets multiple mechanisms of disease progression. Importantly, the ability of m214-sEVs to alter the tumor microenvironment, including potential effects on immune modulation, further enhances their therapeutic relevance. Given their biocompatibility[91,92], targeted delivery capabilities[93-95], and scalable production[96,97], engineered sEVs represent a clinically translatable platform that may improve outcomes for patients with recurrent OC, a population with limited treatment options.

This study lays the groundwork for future translational development and clinical evaluation of miRNA-loaded sEVs as a next-generation therapeutic modality.

Materials and methods

Human Subjects

Human ovarian cancer samples were collected with approval from the Wayne State University Institutional Review Board (IRB-20-07-2521) and the Karmanos Cancer Institute Institutional Review Board (IRB-2013-052). All samples were obtained following informed consent and subsequently de-identified. Research involving human subjects was conducted in full compliance with institutional guidelines and actively reviewed by the respective IRBs.

Cell Lines and Culture Conditions

Human cerebral endothelial cells (CECs) (ACBRI376, Cell Systems) were cultured and passaged in Complete Classic Medium (4Z0-500, Cell Systems). To prepare conditioned medium for sEV isolation, the culture was switched to serum-free medium (SF-4Z0-500, Cell Systems) for 48 hours before collection[18,44].

The cisplatin-resistant human ovarian cancer (OC) cell line A2780cis (RRID:CVCL_1942, Millipore-Sigma, 93112517) was maintained in RPMI-1640 medium supplemented with 10% fetal bovine serum (FBS). To maintain cisplatin resistance, 1 µM cisplatin was added every two passages[98].

Human ovarian cancer stem cell (OCSC) lines, including R182, R2615, and mCherry-OCSC1-F2, were established as previously described [9] and cultured in RPMI-1640 supplemented with 10% FBS, 1% MEM Non-Essential Amino Acids (ThermoFisher, 11140050), 1% HEPES (ThermoFisher, 15630080), and 1% sodium pyruvate (ThermoFisher, 11360070).

OVCAR3/luc cells were generated by transfecting OVCAR3 cells (RRID: CVCL_0465, ATCC HTB-161) with a luciferase expression vector (pLVX-EF1α-IRES-Puro, Clontech), as previously described[18]. These cells were cultured in RPMI-1640 with 10% FBS and selected with 1.2 µg/mL puromycin.

Overexpression of MiRNAs in CECs

Lentiviral constructs carrying the human miR-214-3p precursor (PMIR-214-PA-1, System Biosciences) or a scrambled control (PMIRH000PA-1) were used to generate lentivirus using the Lenti-X Packaging System (Takara)[47]. CECs were infected with the viral supernatant, and stably transduced cells were selected using 1.1 µg/mL puromycin. Puromycin-resistant CECs were expanded and used for downstream experiments [44,47].

Overexpression of YKT6 in OCSCs

Retroviral constructs carrying GFP-YKT6 (pMRXIP-GFP-YKT6) and the corresponding backbone control vector were used to generate retrovirus using pUMVC (Addgene #8449) and pCMV-VSV-G (Addgene #8454) to co-transfect into HEK293T cells. pMRXIP-GFP-YKT6 was a

gift from Noboru Mizushima (Addgene plasmid # 116946 ; http://n2t.net/addgene:116946 ; RRID:Addgene_116946)[99]. pUMVC (Addgene plasmid # 8449 ; http://n2t.net/addgene:8449 ; RRID:Addgene_8449) and pCMV-VSV-G (Addgene plasmid # 8454 ; http://n2t.net/addgene:8454 ; RRID:Addgene_8454) were gifts from Bob Weinberg[100] .

OCSCs were infected with the viral supernatant and selected using puromycin at a concentration of 2 µg/mL. Stable, GFP-positive single-cell clones were isolated, expanded, and maintained for downstream experiments.

The Isolation and Characterization of sEVs

sEVs were isolated from conditioned medium using differential ultracentrifugation, as previously described[14,18,29,47], and were characterized following the MISEV 2018 and 2023 guidelines[14,18,29,47-49]. The concentration and size distribution of CEC-sEVs were analyzed using nanoparticle tracking analysis (NTA) with a NanoSight NS300 (Malvern). The ultrastructural morphology of sEVs was assessed via transmission electron microscopy (TEM; JEM-1400Flash, JEOL) and cryo-electron microscopy (CryoEM; Talos Arctica, ThermoFisher). The expression of sEV surface markers CD63, CD81, and CD9 was evaluated using Western blotting and ExoView analysis, following our previously published protocols[14,29].

The Protein Profile of sEVs and Bioinformatics Analysis

Total proteins were extracted from isolated sEVs and analyzed by mass spectrometry-based proteomics, as described in our previous studies[101,102]. Raw data were processed using Proteome Discoverer 2.4 (Thermo Scientific) and further analyzed with Scaffold software (Proteome Software, Inc.). The raw protein identification results are provided in the Supplemental Excel 1.

Protein enrichment analysis was conducted using the Enrichr gene enrichment analysis tool[103], and Gene Ontology (GO) analysis was performed to identify top-ranked molecular function (MF) categories. First, the enriched proteins are ranked by the spectrum number, and their IDs are converted to the corresponding gene IDs. The gene list was input into the Enrichr website, and the Ontologies database was then applied to perform analysis.

CEC-sEV Labelling and Tracking

To visualize and track CEC-derived sEVs *in vivo*, CECs were transfected with a plasmid encoding a Gluc-Lactadherin fusion construct (a gift from Dr. Takahashi) [57], which directs Gaussia luciferase (Gluc) expression to sEVs via exosomal lactadherin.

For tracking sEV distribution in OC cells, CECs were also transfected with a plasmid encoding CD63-EGFP (pEGFP-CD63, a gift from Paul Luzio; Addgene plasmid #62964), enabling GFP labeling of sEVs via CD63[18,29,47].

Labeled sEVs were administered *in vivo* 2 hours before tissue collection. For detection, immunofluorescent staining was performed on 8 µm cryosections using an anti-GFP antibody (1:500, Cat# 2555, RRID: AB_10692764, Cell Signaling Technology). To determine the subcellular localization of sEVs, immunogold labeling was conducted on 80 nm ultrathin sections using the same primary antibody, followed by 10 nm gold-conjugated streptavidin[18,29,47].

Cell Viability Assays

The cytotoxic effects of sEVs on OC and OCSC cells were assessed using the MTT assay and the CellTox™ Green Cytotoxicity Assay (Promega, G8731), respectively[9,18].

For the MTT assay, OC cells were seeded in 96-well plates and treated with sEVs and chemotherapy drugs for 72 hours. After treatment, 0.5 mg/mL thiazolyl blue tetrazolium bromide (MTT; MilliporeSigma, M2128) was added to each well and incubated for 4 hours. Absorbance was measured using a microplate reader, and cell viability was calculated relative to untreated controls. The IC_{50} was determined by linear regression analysis, representing the concentration of treatment required to inhibit 50% of cell viability.

For the CellTox assay, OCSCs were mixed with CellTox Green dye, seeded into 96-well plates, and treated with sEVs and chemotherapy drugs. Fluorescence intensity, corresponding to the number of dead cells, was measured kinetically over 72 hours using a Bio-Rad plate reader.

Caspase-Glo 3/7 Assay

To assess apoptosis, 10 µg of protein extracted from treated OCSC-R182 cells was diluted in a total volume of 50 µL and mixed with 50 µL of Caspase-Glo 3/7 reagent (Promega). After a 1-hour incubation at room temperature, luminescence was measured using a TD 20/20 Luminometer (Turner Designs, Sunnyvale, CA). Caspase 3/7 activity was calculated relative to untreated controls[104,105].

Transwell Migration Assay

OVCAR3 and OCSC1-F2 cells were resuspended in serum-free RPMI-1640 medium and seeded into Transwell inserts (24-well format) at a density of 2.5 × 10□ cells in 0.5 mL per insert. The lower chambers were filled with 0.75 mL of complete RPMI-1640 medium containing 10% FBS as a chemoattractant[18].

sEVs and chemotherapy drugs were added to the upper chambers and incubated for 24 hours. Migrated OVCAR3 cells were detected using CellTracker Red CMTPX (ThermoFisher, C34552), while migrated OCSC1-F2 cells were identified by mCherry fluorescence.

Animals and the *In Vivo* OC Model

All animal procedures were approved by the Henry Ford Hospital Institutional Animal Care and Use Committee (IACUC) under the following protocols: #1634 (April 16, 2018 – April 15, 2021), #1278 (Feb 16, 2021 – Feb 15, 2024), and #1303 (July 14, 2021 – July 13, 2024).

Female BALB/c nude mice were used to establish an intraperitoneal (i.p.) ovarian cancer (OC) xenograft model. Mice were injected i.p. with 5×10^6 OVCAR3/luc cells one week before treatment initiation[18]. Tumor-bearing mice were randomly assigned to receive carboplatin, sEVs, a combination of carboplatin and sEVs, or PBS as a placebo control.

Tumor burden was monitored weekly using bioluminescence imaging (BLI) with the IVIS Spectrum 200 system (Caliper Life Sciences)[18]. At the endpoint, the mice were sacrificed, the tumors were dissected, and the wet tumor weight was measured.

In situ Hybridization (ISH) of miRNAs

To detect miRNAs in formalin-fixed, paraffin-embedded (FFPE) human OC tumor sections, the miRNAscope assay (ACD Bio-Techne) was performed according to the manufacturer's protocol[106,107]. Pre-designed probes targeting hsa-miR-214-3p (SR-hsa-miR-214-3p-s1), hsa-miR-199a-5p (SR-hsa-miR-199a-5p-s1), a positive control probe for U6 snRNA (SR-RNU6-s1), and a scramble control probe (SR-Scramble-s1) were used. Tissue sections were pretreated with the RNAscope Target Retrieval Kit (322000, ACD Bio-Techne), followed by hydrogen peroxide (H_2O_2) and protease treatment (Pretreat Reagents 322381). Sections were then incubated overnight with the probes. Signal development was performed using the miRNAscope HD Detection Reagents Red (324510). Stained slides were visualized and imaged using a light microscope.

To detect miRNAs in frozen xenograft OC tumor sections from nude mice, fluorescent in situ hybridization (FISH) was performed based on our published protocols and prior studies[108,109]. Sections were fixed with 1-ethyl-3-(3-dimethylaminopropyl) carbodiimide (EDC) to prevent miRNA degradation. miRCURY LNA™ microRNA detection probes (Exiqon) targeting hsa-miR-214-3p, hsa-miR-199a-5p, U6 snRNA, and a scramble control were used. Fluorescent signals were amplified using TSA PLUS Fluorescence Kits (PerkinElmer), and images were acquired using a confocal microscope.

The Isolation of sEVs from the OC Tumor

The t-sEVs were isolated according to the published protocol with some modifications[110,111]. OC xenografts and tumor nodules were dissected from nude mice and rinsed thoroughly with sterile saline to remove blood and debris. Tumor tissues were then minced into small fragments (~1 mm^3) on ice using a sterile razor blade and rinsed again with sterile PBS.

Approximately 0.1 g of tumor tissue was transferred into a 100 mm Petri dish containing 15 mL of OCSC growth medium supplemented with exosome-depleted FBS (Exo-FBS, System Biosciences). After 24 hours of incubation, the supernatant was collected and processed for sEV isolation as described above.

Quantitative Reverse Transcription-Polymerase Chain Reaction

Total RNA from sEVs and OC xenografts was extracted using the miRNeasy Mini Kit (Qiagen, Cat# 217084). RNA was reverse transcribed using the TaqMan MicroRNA Reverse Transcription Kit (Thermo Fisher Scientific, Cat# 4427975), followed by amplification with TaqMan™ MicroRNA Assays specific for: miR-214-3p (MIMAT0000271, Assay ID: 002306), miR-199a-5p (MIMAT0000231, Assay ID: 000498), miR-15b-5p (MIMAT0000417, Assay ID: 000390), miR-16-2-3p (MIMAT0004518, Assay ID: 002171). U6 snRNA (MIM180692, Assay ID: 001973) was used as the endogenous control. qRT-PCR was performed using the following thermal cycling conditions: 95°C for 20 seconds (initial denaturation), followed by 40 cycles of 95°C for 1 second and 60°C for 20 seconds. Relative miRNA expression levels were calculated using the 2^−ΔΔCt method, normalized to U6[18,47].

Western Blotting

Proteins were extracted from sEVs, OC cells, or xenograft tumor tissues, and analyzed by Western blotting as previously described in our published protocols[18,47]. Briefly, primary antibodies were incubated with membranes overnight at 4°C, followed by incubation with secondary antibodies for 2 hours at room temperature (RT). Protein bands were visualized using ECL Western blotting substrates (Thermo Fisher Scientific), and band intensity was quantified using AlphaView SA software (version 3.4.0, Bio-Techne). The following primary antibodies were used:

Name	Supplier, Catalog #	RRID	Dilution
CD63	Santa CruZ, sc-5275	RRID:AB_627877	1:500
CD81	Abcam, ab109201	RRID:AB_10866464	1:1000
CD9	Abcam, ab223052	RRID:AB_2922392	1:1000
calnexin	Biolegend, 699041	-	1:1000
TLR4	Novus, NBP2-27149	RRID:AB_2936296	1:1000
β-catenin	Santa Cruz, SC-1496	RRID:AB_1563968	1:1000
Caspase3, cleaved	Cell Signaling, 9661	RRID:AB_2341188	1:1000
MMP2	MilliporeSigma, MAB13405	RRID:AB_94120	1:1000
MMP9	Novus, NBP2-41233	RRID:AB_3302960	1:1000

YKT6	Abclonal, A17083	RRID:AB_2772927	1:1000
Integrin β1	Santa Cruz, sc-8978	RRID:AB_2130101	1:1000
β-actin	Abcam, ab6276	RRID:AB_2223210	1:5000

Statistical Analysis

Statistical analyses were performed using GraphPad Prism (version 8.2.1, GraphPad Software). The following tests were applied:

One-way ANOVA with Tukey's multiple comparisons test for comparisons among more than two groups;

Two-way repeated measures ANOVA for comparisons of OC tumor growth over time between treatment groups;

Unpaired two-tailed Student's t-test for comparisons between two groups.

Data are presented as mean ± standard error of the mean (SEM). A P-value < 0.05 was considered statistically significant.

Figures

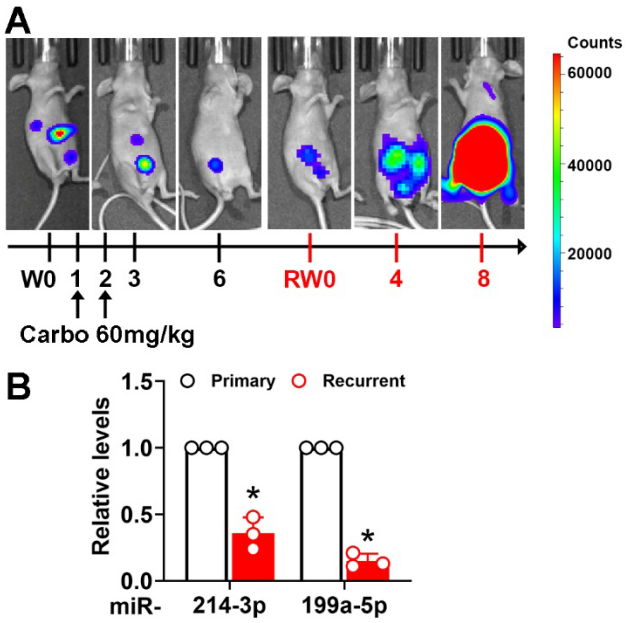

Figure 1. Tumor Recurrence in a Xenograft Model of OC and Downregulation of miR-214-3p and miR-199a-5p in recurrent tumors

(A) Representative BLI of mice bearing intraperitoneal OVCAR3/luc xenografts treated with carboplatin (60 mg/kg) at weeks 1 (W1) and 2 (W2) post-implantation. Tumor recurrence was first detected and designated as recurrence week 0 (RW0) and progressed through recurrence weeks 4 (RW4) and 8 (RW8). The color scale reflects photon flux intensity (photons/sec/cm^2). **(B)** Quantitative RT-PCR analysis of miR-214-3p and miR-199a-5p expression in primary tumors (W2) compared to recurrent tumors (RW4). Data are presented as mean ± SEM. *$p < 0.05$ versus primary group, determined by one-way ANOVA.

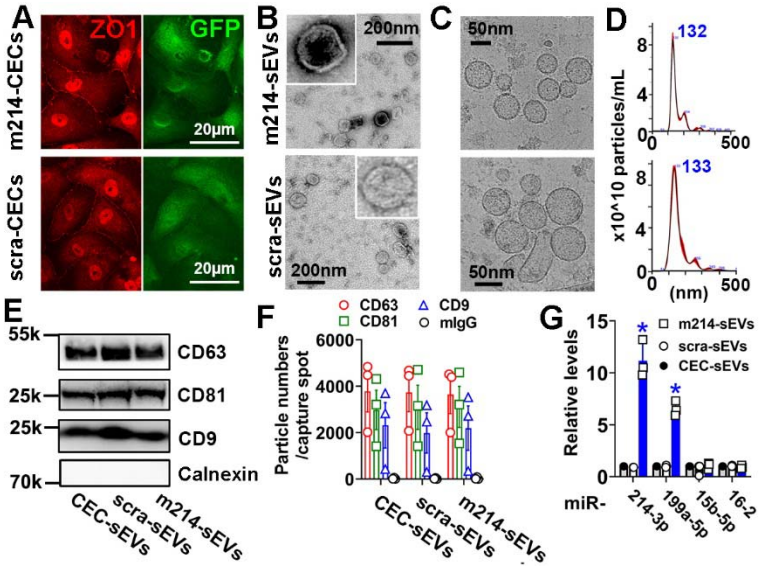

Figure 2: Characterization of Engineered CEC-Derived sEVs Enriched with miR-214-3p

(**A**) Representative fluorescence images of CECs transduced with either miR-214-3p (m214-CECs) or scrambled control (scra-CECs) show robust GFP expression and preserved endothelial phenotype as indicated by the tight junction marker ZO1. (**B, C**) Representative TEM and cryo-EM images with enlarged views show isolated sEVs from m214-CECs (m214-sEVs) and scra-CECs (scra-sEVs). (**D**) Nanoparticle tracking analysis (NTA) results show comparable size distributions of m214-sEVs and scra-sEVs. (**E**) Western blot results demonstrate the presence of tetraspanin markers (CD63, CD81, CD9) and the absence of the endoplasmic reticulum marker calnexin, indicating the purity of vesicle preparations. (**F**) ExoView-based quantification of $CD63^+$, $CD81^+$, and $CD9^+$ particle counts across EV preparations. (**G**) Quantitative RT-PCR analysis of miR-214-3p, miR-199a-5p, miR-15b-3p, and miR-16-2 in the different EV samples. $p < 0.05$ vs. scra-sEVs, assessed by one-way ANOVA.

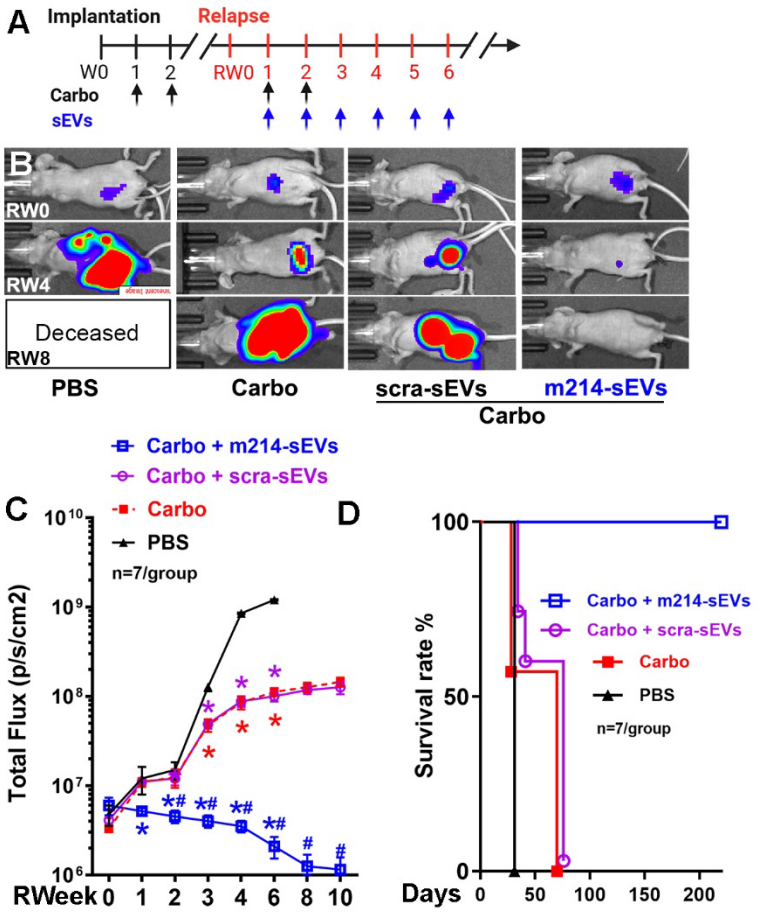

Figure 3. m214-sEVs Enhance Carboplatin Therapeutic Efficacy and Prolong Survival in a Recurrent OC Model. (**A**) Schematic of the treatment timeline for the survival study. Mice bearing intraperitoneal OVCAR3/luc tumors were treated with carboplatin (Carbo, 60 mg/kg, black arrows), and/or sEVs (scra-sEVs or m214-sEVs, blue arrows) beginning at the time of tumor recurrence (RW1). (**B**) Representative BLI of mice show tumor burden across the treatment groups. (**C**) Quantification of BLI signal over time demonstrates reduced tumor progression in the Carbo + m214-sEV group. *$p < 0.05$ vs. PBS; #$p < 0.05$ vs. Carbo alone, assessed by two-way ANOVA with Tukey's post hoc test. (**D**) Kaplan–Meier survival analysis reveals significantly prolonged survival in mice treated with Carbo + m214-sEVs compared to other groups. Log-rank (Mantel–Cox) test results: $p < 0.05$ for Carbo vs. PBS and Carbo + scra-sEVs vs. PBS; $p < 0.001$ for Carbo + m214-sEVs vs. Carbo and Carbo + m214-sEVs vs. PBS; non-significant for Carbo vs. Carbo + scra-sEVs.

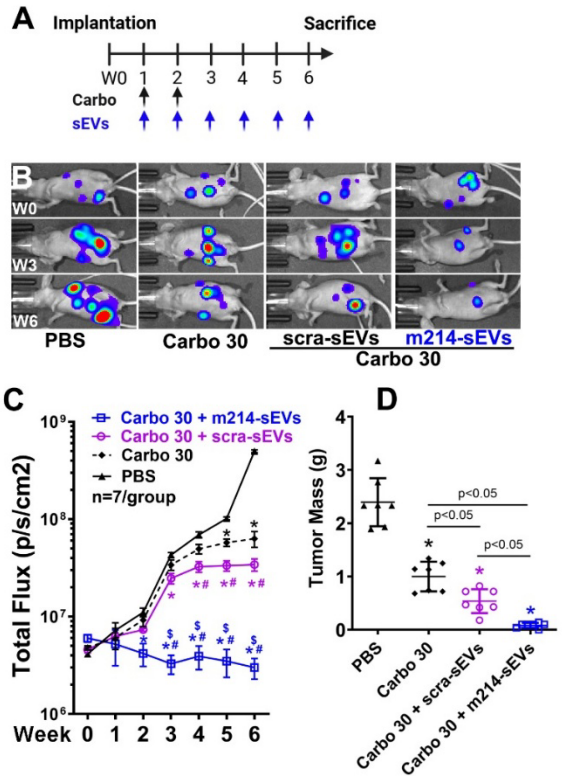

Figure 4. m214-sEVs Enhance the Therapeutic Efficacy of Low-Dose Carboplatin in Primary Ovarian Cancer

(**A**) Schematic of the treatment timeline. Mice bearing intraperitoneal OVCAR3/luc tumors received low-dose carboplatin (Carbo, 30 mg/kg; black arrows) and/or sEVs (scra-sEVs or m214-sEVs; blue arrows), starting one week post-implantation (W1). Mice were sacrificed at week 6 (W6) for endpoint analysis. (**B**) Representative BLI of mice from each treatment group. (**C**) Quantification of BLI signal over time showed differences in tumor progression among groups. *$p < 0.05$ vs. PBS; #$p < 0.05$ vs. Carbo 30 alone; \$$p < 0.05$ vs. Carbo + scra-sEVs; assessed by two-way ANOVA with Tukey's post hoc test. (**D**) Endpoint quantification of tumor mass at W6. *$p < 0.05$ vs. PBS; determined by one-way ANOVA with multiple comparisons.

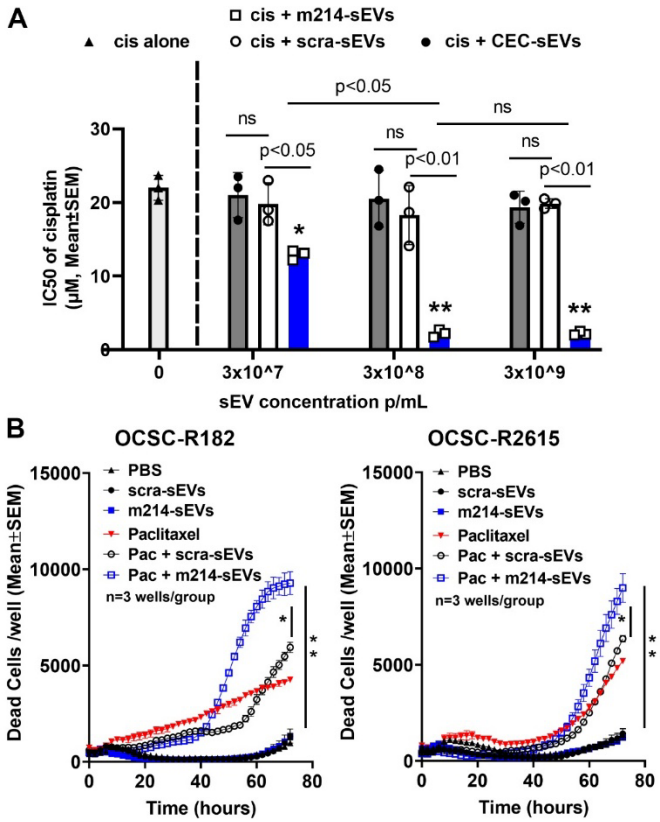

Figure 5. m214-sEVs Sensitize Chemoresistant OC Cells to Cisplatin and Paclitaxel. (**A**) IC_{50} values of cisplatin in A2780cis cells treated with increasing concentrations of sEVs (3×10□, 3×10□, or 3×10□ particles/mL) in combination with cisplatin. (**B**) Quantitative analysis of cytotoxicity in chemoresistant OCSC lines R182 and R2615, treated with paclitaxel (Pac; 20 µM) in combination with sEVs (3×10□ particles/mL) over 72 hours. Cell death was assessed using real-time CellTox Green assays. Data are presented as mean ± SEM from n = 3 wells per group. *p < 0.05, **p < 0.01 by one-way ANOVA with Tukey's post hoc test.

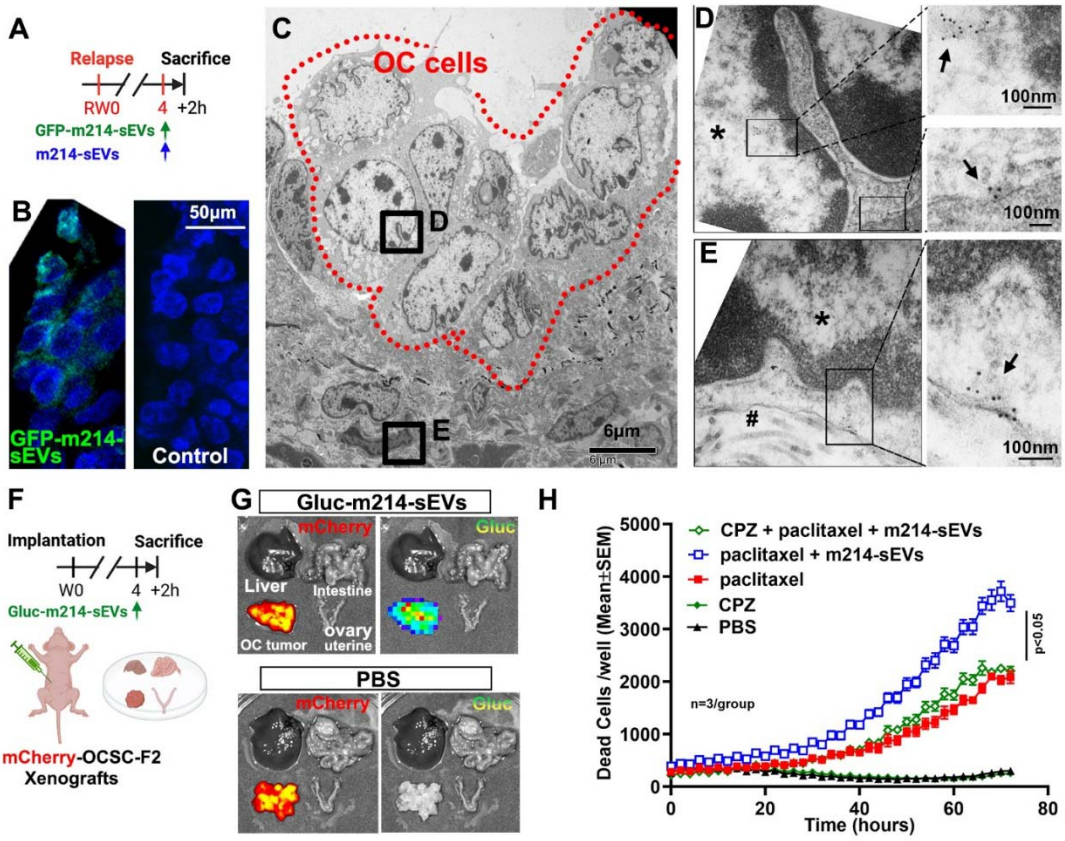

Figure 6. Biodistribution, Cellular Uptake, and Functional Impact of m214-sEVs in Recurrent OC.

(**A**) Schematic of the experimental timeline. Mice bearing relapsed OC were intraperitoneally injected with either GFP-labeled m214-sEVs or unlabeled m214-sEVs and sacrificed 2 hours post-injection. (**B**) Immunofluorescence images of relapsed OC nodules showed strong GFP signal in tumors from mice treated with GFP-m214-sEVs, while no GFP signal was detected in the unlabeled control group. (**C**) Representative TEM image of a relapsed OC nodule, with tumor cells outlined by red dashed lines. (**D**) Higher-magnification view of the boxed region in (C) revealed immunogold-labeled GFP particles localized to both the nucleus (*) and cytoplasm of tumor cells. (**E**) Adjacent stromal region from the same nodule showed immunogold-labeled particles within fibroblast cytoplasm, closely associated with collagen fibers (#). (**F**) Schematic of the experimental design for Gluc-m214-sEV tracking. Mice bearing mCherry^{+} OCSC1-F2 xenografts were intraperitoneally injected with Gluc-labeled m214-sEVs (Gluc-m214-sEVs), and tissues were harvested 2 hours later. (**G**) *Ex vivo* BLI demonstrated preferential accumulation of Gluc-m214-sEVs in OC tumor tissues, with minimal signal detected in liver, ovary, or intestine. (**H**) Real-time CellTox Green cytotoxicity assay demonstrated the effect of

pretreatment with chlorpromazine (CPZ) prior to paclitaxel and/or m214-sEVs in OCSC-F182 cells. *$p < 0.05$, assessed by one-way ANOVA with Tukey's post hoc test; n = 3 wells/group.

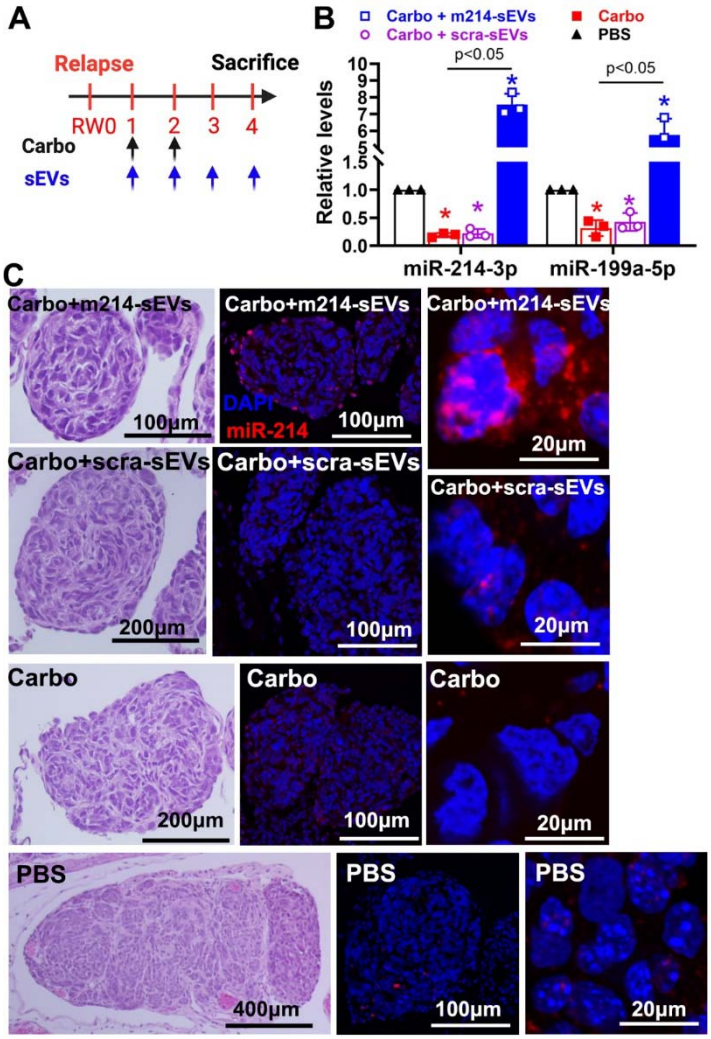

Figure 7. Combination Treatment with m214-sEVs and Carboplatin Enhances Intratumoral miR-214-3p/199a-5p Levels in Relapsed OC

(**A**) Schematic of the treatment timeline. Mice bearing relapsed OC were treated with carboplatin (Carbo, black arrows) and/or small extracellular vesicles (sEVs, blue arrows), and tumors were collected at relapse week 4 (RW4). (**B**) qRT-PCR analysis of tumor tissues showed significantly elevated levels of miR-214-3p and miR-199a-5p in the combination treatment group (m214-sEVs + Carbo) compared to all other groups. *$p < 0.05$, one-way ANOVA with Tukey's post hoc test. (**C**) Representative H&E staining and fluorescent in situ hybridization (ISH) images of relapsed OC nodules revealed increased miR-214-3p expression (red signal) in OC cells following combination treatment with m214-sEVs and carboplatin.

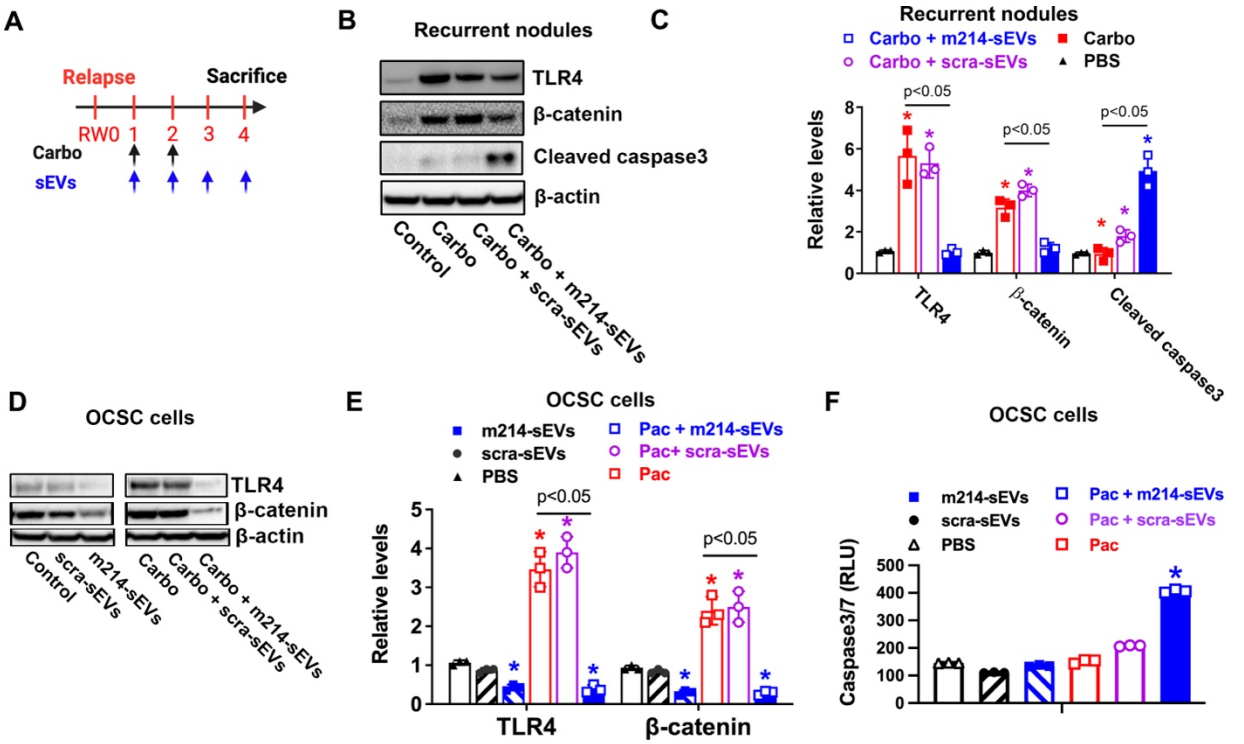

Figure 8. Combined m214-sEV and Chemotherapy Treatment Downregulates TLR4/β-Catenin and Promotes Apoptosis in OC

(**A**) Schematic of the treatment schedule. Mice bearing relapsed OC tumors were treated with carboplatin (black arrows) and/or sEVs (blue arrows). Tumors were harvested four weeks after recurrence. (**B, C**) Representative Western blots (**B**) and corresponding quantitative analysis (**C**) of tumor lysates showed reduced expression of TLR4 and β-catenin, and increased levels of cleaved caspase-3 in mice receiving the combination treatment with m214-sEVs and carboplatin. *$p < 0.05$, assessed by one-way ANOVA with Tukey's post hoc test. (**D, E**) Western blot (**D**) and quantitative analysis (**E**) of TLR4 and β-catenin expression in OCSC-R182 cells following indicated treatments. (**F**) Caspase-3/7 activity assay in OCSC1-F2 cells showed increased apoptosis following combined treatment with m214-sEVs and paclitaxel (Pac). *$p < 0.05$ vs. Pac or other treatment groups, assessed by one-way ANOVA.

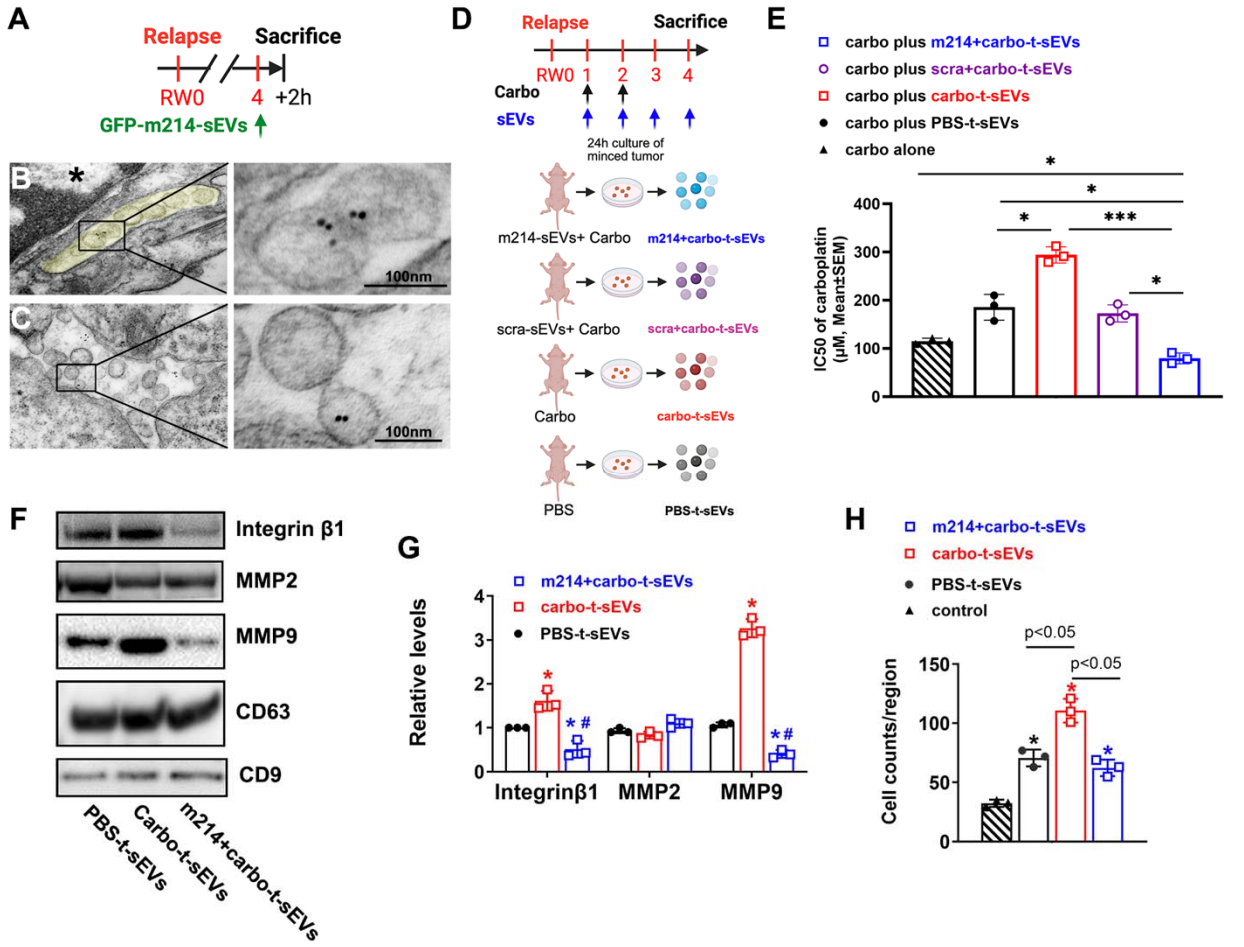

Figure 9. m214-sEVs Change Secondary t-sEV Composition and Abrogate Its Pro-metastatic Effects in OC.

(**A**) Schematic illustrating the in vivo treatment regimen and timeline for tissue collection. (**B, C**) Representative TEM images of relapsed OC tissue showed immunogold-labeled GFP-m214-sEVs localized within MVBs (**B**) and in the extracellular space (**C**). (**D**) Schematic of experimental design: tumor-derived sEVs (t-sEVs) were isolated from minced tumor tissues of mice treated under four different conditions. (**E**) Quantification of carboplatin IC_{50} values in mCherry^{+} OCSC-F2 cells following treatment with various t-sEVs preparations. (**F, G**) Western blot analysis (**F**) and corresponding quantification (**G**) of t-sEV cargo proteins, including Integrin β1, MMP2, MMP9, CD63, and CD9. (**H**) Quantitative results of transwell invasion assays in OCSC-F2 cells treated with t-sEV. *p < 0.05, **p < 0.01, ***p < 0.001 by one-way ANOVA with Tukey's post hoc test.

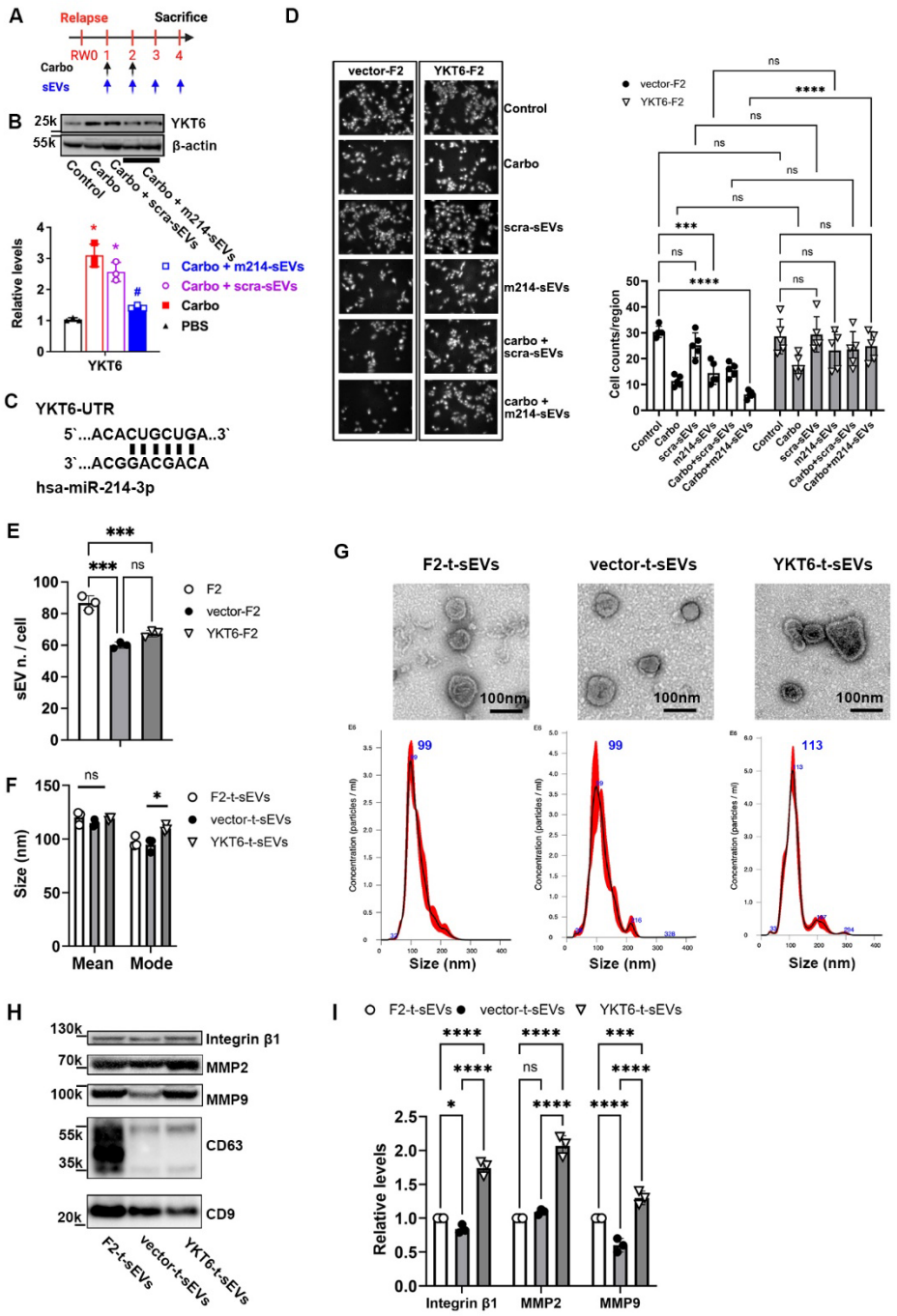

Figure 10. Functional Role of YKT6 in Cell Motility and sEV Cargo in OC.

(**A**) Schematic of the treatment timeline showing administration of carboplatin (Carbo) and/or sEV, followed by tissue collection at relapse week 4 (RW4). (**B**) Representative Western blot and corresponding quantification of YKT6 protein levels in recurrent OC xenografts. (**C**) Schematic illustrating the predicted miR-214-3p binding site within the 3'UTR of YKT6 mRNA. (**D**) Representative images and quantification of transwell migration assays comparing YKT6-

overexpressing (YKT6-F2) and control vector-transduced (vector-F2) cells. (**E**) Quantification of sEV secretion per cell, measured by NTA, in YKT6-F2, vector-F2, and F2 parental cells following the indicated treatments. (**F**) Quantification of mean and mode sizes of t-sEVs from different cell types. (**G**) Representative TEM images and corresponding NTA profiles showing t-sEV morphology and size distribution. (**H, I**) Representative Western blot (**H**) and quantification (**I**) of protein cargo in three types of t-sEVs. *$p < 0.05$, ***$p < 0.001$, ****$p < 0.0001$, ns = not significant; assessed by one-way ANOVA with Tukey's post hoc test.

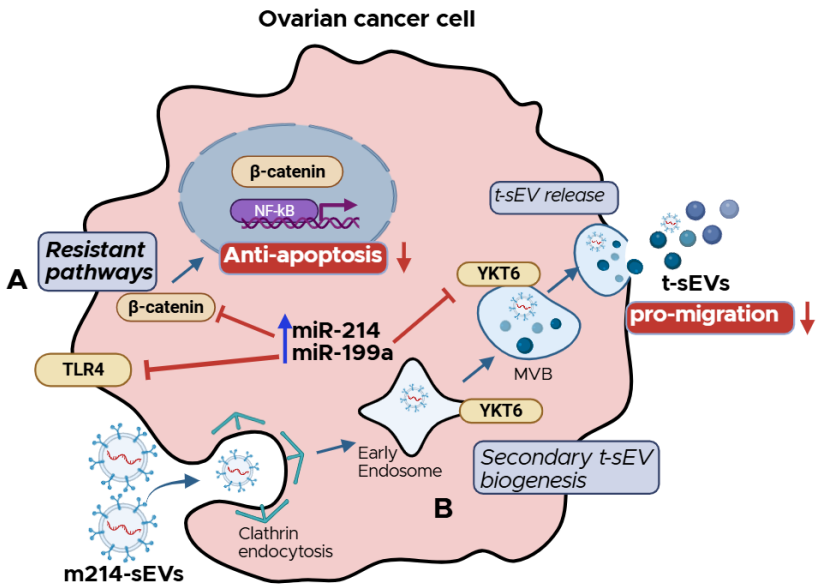

Fig. 11. Schematic Illustrating the Proposed Molecular and Cellular Mechanisms by which m214-sEVs Exert Therapeutic Effects in Recurrent OC.

(**A**) Following clathrin-mediated endocytosis, m214-sEVs deliver miR-214-3p and miR-199a-5p into ovarian cancer cells, resulting in the downregulation of chemoresistance-associated genes, TLR4 and β-catenin. This suppression inhibits anti-apoptotic signaling pathways and restores sensitivity to chemotherapy. (**B**) m214-sEVs also downregulate YKT6, a SNARE protein involved in MVB trafficking, leading to altered biogenesis and protein cargo composition of secondary tumor-derived sEVs (t-sEVs), contributing to reduced tumor invasiveness and recurrence. Created in BioRender (BioRender.com/2fgsdlc).

References:

1. Mor G, Yin G, Chefetz I, Yang Y, Alvero A. Ovarian cancer stem cells and inflammation. *Cancer Biol Ther*. 2011;11:708-713. doi: 10.4161/cbt.11.8.14967
2. Liu M, Mor G, Cheng H, Xiang X, Hui P, Rutherford T, Yin G, Rimm DL, Holmberg J, Alvero A, et al. High frequency of putative ovarian cancer stem cells with CD44/CK19 coexpression is associated with decreased progression-free intervals in patients with recurrent epithelial ovarian cancer. *Reprod Sci*. 2013;20:605-615. doi: 10.1177/1933719112461183
3. Adzibolosu N, Alvero AB, Ali-Fehmi R, Gogoi R, Corey L, Tedja R, Chehade H, Gogoi V, Morris R, Anderson M, et al. Immunological modifications following chemotherapy are associated with delayed recurrence of ovarian cancer. *Front Immunol*. 2023;14:1204148. doi: 10.3389/fimmu.2023.1204148
4. Matulonis UA, Sood AK, Fallowfield L, Howitt BE, Sehouli J, Karlan BY. Ovarian cancer. *Nat Rev Dis Primers*. 2016;2:16061. doi: 10.1038/nrdp.2016.61
5. Christie EL, Bowtell DDL. Acquired chemotherapy resistance in ovarian cancer. *Ann Oncol*. 2017;28:viii13-viii15. doi: 10.1093/annonc/mdx446
6. Choe S, Jeon M, Yoon H. Advanced Therapeutic Approaches for Metastatic Ovarian Cancer. *Cancers (Basel)*. 2025;17. doi: 10.3390/cancers17050788
7. Lupia M, Cavallaro U. Ovarian cancer stem cells: still an elusive entity? *Mol Cancer*. 2017;16:64. doi: 10.1186/s12943-017-0638-3
8. Alvero AB, Heaton A, Lima E, Pitruzzello M, Sumi N, Yang-Hartwich Y, Cardenas C, Steinmacher S, Silasi DA, Brown D, et al. TRX-E-002-1 Induces c-Jun-Dependent Apoptosis in Ovarian Cancer Stem Cells and Prevents Recurrence In Vivo. *Mol Cancer Ther*. 2016;15:1279-1290. doi: 10.1158/1535-7163.MCT-16-0005
9. Craveiro V, Yang-Hartwich Y, Holmberg JC, Joo WD, Sumi NJ, Pizzonia J, Griffin B, Gill SK, Silasi DA, Azodi M, et al. Phenotypic modifications in ovarian cancer stem cells following Paclitaxel treatment. *Cancer Med*. 2013;2:751-762. doi: 10.1002/cam4.115
10. Chefetz I, Alvero AB, Holmberg JC, Lebowitz N, Craveiro V, Yang-Hartwich Y, Yin G, Squillace L, Gurrea Soteras M, Aldo P, et al. TLR2 enhances ovarian cancer stem cell self-renewal and promotes tumor repair and recurrence. *Cell Cycle*. 2013;12:511-521. doi: 10.4161/cc.23406
11. Fang Y, Xiao X, Wang J, Dasari S, Pepin D, Nephew KP, Zamarin D, Mitra AK. Cancer associated fibroblasts serve as an ovarian cancer stem cell niche through noncanonical Wnt5a signaling. *NPJ Precis Oncol*. 2024;8:7. doi: 10.1038/s41698-023-00495-5
12. Zhang M, Chen Z, Wang Y, Zhao H, Du Y. The Role of Cancer-Associated Fibroblasts in Ovarian Cancer. *Cancers (Basel)*. 2022;14. doi: 10.3390/cancers14112637
13. Fu X, Li Y, Alvero A, Li J, Wu Q, Xiao Q, Peng Y, Hu Y, Li X, Yan W, et al. MicroRNA-222-3p/GNAI2/AKT axis inhibits epithelial ovarian cancer cell growth and associates with good overall survival. *Oncotarget*. 2016;7:80633-80654. doi: 10.18632/oncotarget.13017
14. Zhang Y, Tedja R, Millman M, Wong T, Fox A, Chehade H, Gershater M, Adzibolosu N, Gogoi R, Anderson M, et al. Adipose-derived exosomal miR-421 targets CBX7 and promotes metastatic potential in ovarian cancer cells. *J Ovarian Res*. 2023;16:233. doi: 10.1186/s13048-023-01312-0
15. Li Y, Fang Y, Liu Y, Yang X. MicroRNAs in ovarian function and disorders. *J Ovarian Res*. 2015;8:51. doi: 10.1186/s13048-015-0162-2
16. Ravegnini G, De Iaco P, Gorini F, Dondi G, Klooster I, De Crescenzo E, Bovicelli A, Hrelia P, Perrone AM, Angelini S. Role of Circulating miRNAs in Therapeutic Response in Epithelial Ovarian Cancer: A Systematic Revision. *Biomedicines*. 2021;9. doi: 10.3390/biomedicines9101316

17. Kim YW, Kim EY, Jeon D, Liu JL, Kim HS, Choi JW, Ahn WS. Differential microRNA expression signatures and cell type-specific association with Taxol resistance in ovarian cancer cells. *Drug Des Devel Ther*. 2014;8:293-314. doi: 10.2147/DDDT.S51969
18. Zhang Y, Li C, Qin Y, Cepparulo P, Millman M, Chopp M, Kemper A, Szalad A, Lu X, Wang L, et al. Small extracellular vesicles ameliorate peripheral neuropathy and enhance chemotherapy of oxaliplatin on ovarian cancer. *J Extracell Vesicles*. 2021;10:e12073. doi: 10.1002/jev2.12073
19. Ravindran F, Mhatre A, Koroth J, Narayan S, Choudhary B. Curcumin modulates cell type-specific miRNA networks to induce cytotoxicity in ovarian cancer cells. *Life Sci*. 2023;334:122224. doi: 10.1016/j.lfs.2023.122224
20. Muys BR, Sousa JF, Placa JR, de Araujo LF, Sarshad AA, Anastasakis DG, Wang X, Li XL, de Molfetta GA, Ramao A, et al. miR-450a Acts as a Tumor Suppressor in Ovarian Cancer by Regulating Energy Metabolism. *Cancer Res*. 2019;79:3294-3305. doi: 10.1158/0008-5472.CAN-19-0490
21. Wang F, Chang JT, Kao CJ, Huang RS. High Expression of miR-532-5p, a Tumor Suppressor, Leads to Better Prognosis in Ovarian Cancer Both In Vivo and In Vitro. *Mol Cancer Ther*. 2016;15:1123-1131. doi: 10.1158/1535-7163.MCT-15-0943
22. Zhang Q, Zhang S. miR-214 promotes radioresistance in human ovarian cancer cells by targeting PETN. *Biosci Rep*. 2017;37. doi: 10.1042/BSR20170327
23. Yang H, Kong W, He L, Zhao JJ, O'Donnell JD, Wang J, Wenham RM, Coppola D, Kruk PA, Nicosia SV, et al. MicroRNA expression profiling in human ovarian cancer: miR-214 induces cell survival and cisplatin resistance by targeting PTEN. *Cancer Res*. 2008;68:425-433. doi: 10.1158/0008-5472.CAN-07-2488
24. Nam EJ, Yoon H, Kim SW, Kim H, Kim YT, Kim JH, Kim JW, Kim S. MicroRNA expression profiles in serous ovarian carcinoma. *Clin Cancer Res*. 2008;14:2690-2695. doi: 10.1158/1078-0432.CCR-07-1731
25. Liu Y, Zhou H, Ma L, Hou Y, Pan J, Sun C, Yang Y, Zhang J. MiR-214 suppressed ovarian cancer and negatively regulated semaphorin 4D. *Tumour Biol*. 2016;37:8239-8248. doi: 10.1007/s13277-015-4708-0
26. Chen R, Alvero AB, Silasi DA, Kelly MG, Fest S, Visintin I, Leiser A, Schwartz PE, Rutherford T, Mor G. Regulation of IKKbeta by miR-199a affects NF-kappaB activity in ovarian cancer cells. *Oncogene*. 2008;27:4712-4723. doi: 10.1038/onc.2008.112
27. Kelly MG, Alvero AB, Chen R, Silasi DA, Abrahams VM, Chan S, Visintin I, Rutherford T, Mor G. TLR-4 signaling promotes tumor growth and paclitaxel chemoresistance in ovarian cancer. *Cancer Res*. 2006;66:3859-3868. doi: 10.1158/0008-5472.CAN-05-3948
28. Mathieu M, Martin-Jaular L, Lavieu G, Thery C. Specificities of secretion and uptake of exosomes and other extracellular vesicles for cell-to-cell communication. *Nat Cell Biol*. 2019;21:9-17. doi: 10.1038/s41556-018-0250-9
29. Wang M, Wang W, Chopp M, Zhang ZG, Zhang Y. Therapeutic and diagnostic potential of extracellular vesicle (EV)-mediated intercellular transfer of mitochondria and mitochondrial components. *J Cereb Blood Flow Metab*. 2025:271678X251338971. doi: 10.1177/0271678X251338971
30. Tkach M, Thery C. Communication by Extracellular Vesicles: Where We Are and Where We Need to Go. *Cell*. 2016;164:1226-1232. doi: 10.1016/j.cell.2016.01.043
31. Zhang ZG, Buller B, Chopp M. Exosomes - beyond stem cells for restorative therapy in stroke and neurological injury. *Nat Rev Neurol*. 2019;15:193-203. doi: 10.1038/s41582-018-0126-4
32. Zhang J, Li S, Li L, Li M, Guo C, Yao J, Mi S. Exosome and exosomal microRNA: trafficking, sorting, and function. *Genomics Proteomics Bioinformatics*. 2015;13:17-24. doi: 10.1016/j.gpb.2015.02.001

33. Murphy DE, de Jong OG, Evers MJW, Nurazizah M, Schiffelers RM, Vader P. Natural or Synthetic RNA Delivery: A Stoichiometric Comparison of Extracellular Vesicles and Synthetic Nanoparticles. *Nano Lett*. 2021. doi: 10.1021/acs.nanolett.1c00094
34. de Jong OG, Murphy DE, Mager I, Willms E, Garcia-Guerra A, Gitz-Francois JJ, Lefferts J, Gupta D, Steenbeek SC, van Rheenen J, et al. A CRISPR-Cas9-based reporter system for single-cell detection of extracellular vesicle-mediated functional transfer of RNA. *Nat Commun*. 2020;11:1113. doi: 10.1038/s41467-020-14977-8
35. Zheng W, He R, Liang X, Roudi S, Bost J, Coly PM, van Niel G, Andaloussi SEL. Cell-specific targeting of extracellular vesicles through engineering the glycocalyx. *J Extracell Vesicles*. 2022;11:e12290. doi: 10.1002/jev2.12290
36. Kalluri R, LeBleu VS. The biology, function, and biomedical applications of exosomes. *Science*. 2020;367. doi: 10.1126/science.aau6977
37. Behbahani GD, Khani S, Hosseini HM, Abbaszadeh-Goudarzi K, Nazeri S. The role of exosomes contents on genetic and epigenetic alterations of recipient cancer cells. *Iran J Basic Med Sci*. 2016;19:1031-1039.
38. Qian Z, Shen Q, Yang X, Qiu Y, Zhang W. The Role of Extracellular Vesicles: An Epigenetic View of the Cancer Microenvironment. *Biomed Res Int*. 2015;2015:649161. doi: 10.1155/2015/649161
39. Zhang L, Yu D. Exosomes in cancer development, metastasis, and immunity. *Biochim Biophys Acta Rev Cancer*. 2019;1871:455-468. doi: 10.1016/j.bbcan.2019.04.004
40. Guo Y, Ji X, Liu J, Fan D, Zhou Q, Chen C, Wang W, Wang G, Wang H, Yuan W, et al. Effects of exosomes on pre-metastatic niche formation in tumors. *Mol Cancer*. 2019;18:39. doi: 10.1186/s12943-019-0995-1
41. Zhou J, Tan X, Tan Y, Li Q, Ma J, Wang G. Mesenchymal Stem Cell Derived Exosomes in Cancer Progression, Metastasis and Drug Delivery: A Comprehensive Review. *J Cancer*. 2018;9:3129-3137. doi: 10.7150/jca.25376
42. Jahangiri B, Khalaj-Kondori M, Asadollahi E, Purrafee Dizaj L, Sadeghizadeh M. MSC-Derived exosomes suppress colorectal cancer cell proliferation and metastasis via miR-100/mTOR/miR-143 pathway. *Int J Pharm*. 2022;627:122214. doi: 10.1016/j.ijpharm.2022.122214
43. Setua S, Shabir S, Shaji P, Bulnes AM, Dhasmana A, Holla S, Mittal NK, Sahoo N, Saini T, Giorgianni F, et al. Exosomes derived from tumor adjacent fibroblasts efficiently target pancreatic tumors. *Acta Pharm Sin B*. 2024;14:3009-3026. doi: 10.1016/j.apsb.2024.04.003
44. Semaan L, Zeng Q, Lu Y, Zhang Y, Zreik MM, Chamseddine MB, Chopp M, Zhang ZG, Moonka D. MicroRNA-214 enriched exosomes from human cerebral endothelial cells (hCEC) sensitize hepatocellular carcinoma to anti-cancer drugs. *Oncotarget*. 2021;12:185-198. doi: 10.18632/oncotarget.27879
45. Li D, Williams JI, Pietras RJ. Squalamine and cisplatin block angiogenesis and growth of human ovarian cancer cells with or without HER-2 gene overexpression. *Oncogene*. 2002;21:2805-2814. doi: 10.1038/sj.onc.1205410
46. Boven E, van der Vijgh WJ, Nauta MM, Schluper HM, Pinedo HM. Comparative activity and distribution studies of five platinum analogues in nude mice bearing human ovarian carcinoma xenografts. *Cancer Res*. 1985;45:86-90.
47. Zhang Y, Liu Z, Chopp M, Millman M, Li Y, Cepparulo P, Kemper A, Li C, Zhang L, Zhang ZG. Small extracellular vesicles derived from cerebral endothelial cells with elevated microRNA 27a promote ischemic stroke recovery. *Neural Regen Res*. 2025;20:224-233. doi: 10.4103/NRR.NRR-D-22-01292
48. Welsh JA, Goberdhan DCI, O'Driscoll L, Buzas EI, Blenkiron C, Bussolati B, Cai H, Di Vizio D, Driedonks TAP, Erdbrugger U, et al. Minimal information for studies of extracellular vesicles

(MISEV2023): From basic to advanced approaches. *J Extracell Vesicles*. 2024;13:e12404. doi: 10.1002/jev2.12404
49. Thery C, Witwer KW, Aikawa E, Alcaraz MJ, Anderson JD, Andriantsitohaina R, Antoniou A, Arab T, Archer F, Atkin-Smith GK, et al. Minimal information for studies of extracellular vesicles 2018 (MISEV2018): a position statement of the International Society for Extracellular Vesicles and update of the MISEV2014 guidelines. *J Extracell Vesicles*. 2018;7:1535750. doi: 10.1080/20013078.2018.1535750
50. Fotopoulou C. Limitations to the use of carboplatin-based therapy in advanced ovarian cancer. *EJC Suppl*. 2014;12:13-16. doi: 10.1016/S1359-6349(15)70005-4
51. Colby C, Koziol S, McAfee SL, Yeap B, Spitzer TR. High-dose carboplatin and regimen-related toxicity following autologous bone marrow transplant. *Bone Marrow Transplant*. 2002;29:467-472. doi: 10.1038/sj.bmt.1703417
52. Li J, Hu H, He J, Hu Y, Liu M, Cao B, Chen D, Ye X, Zhang J, Zhang Z, et al. Effective sequential combined therapy with carboplatin and a CDC7 inhibitor in ovarian cancer. *Transl Oncol*. 2024;39:101825. doi: 10.1016/j.tranon.2023.101825
53. Zhou S, Wang R, Xiao H. Adipocytes induce the resistance of ovarian cancer to carboplatin through ANGPTL4. *Oncol Rep*. 2020;44:927-938. doi: 10.3892/or.2020.7647
54. Pokhriyal R, Hariprasad R, Kumar L, Hariprasad G. Chemotherapy Resistance in Advanced Ovarian Cancer Patients. *Biomark Cancer*. 2019;11:1179299X19860815. doi: 10.1177/1179299X19860815
55. Polajzer S, Cerne K. Precision Medicine in High-Grade Serous Ovarian Cancer: Targeted Therapies and the Challenge of Chemoresistance. *Int J Mol Sci*. 2025;26. doi: 10.3390/ijms26062545
56. Steffensen KD, Alvero AB, Yang Y, Waldstrom M, Hui P, Holmberg JC, Silasi DA, Jakobsen A, Rutherford T, Mor G. Prevalence of epithelial ovarian cancer stem cells correlates with recurrence in early-stage ovarian cancer. *J Oncol*. 2011;2011:620523. doi: 10.1155/2011/620523
57. Takahashi Y, Nishikawa M, Takakura Y. In Vivo Tracking of Extracellular Vesicles in Mice Using Fusion Protein Comprising Lactadherin and Gaussia Luciferase. *Methods Mol Biol*. 2017;1660:245-254. doi: 10.1007/978-1-4939-7253-1_20
58. Tu C, Du Z, Zhang H, Feng Y, Qi Y, Zheng Y, Liu J, Wang J. Endocytic pathway inhibition attenuates extracellular vesicle-induced reduction of chemosensitivity to bortezomib in multiple myeloma cells. *Theranostics*. 2021;11:2364-2380. doi: 10.7150/thno.47996
59. Pang B, Qiao L, Wang S, Guo X, Xie Y, Han L. MiR-214-3p plays a protective role in diabetic neuropathic rats by regulating Nav1.3 and TLR4. *Cell Biol Int*. 2021;45:2294-2303. doi: 10.1002/cbin.11677
60. Deng ZF, Zheng HL, Chen JG, Luo Y, Xu JF, Zhao G, Lu JJ, Li HH, Gao SQ, Zhang DZ, et al. miR-214-3p Targets beta-Catenin to Regulate Depressive-like Behaviors Induced by Chronic Social Defeat Stress in Mice. *Cereb Cortex*. 2019;29:1509-1519. doi: 10.1093/cercor/bhy047
61. Alvero AB, Chen R, Fu HH, Montagna M, Schwartz PE, Rutherford T, Silasi DA, Steffensen KD, Waldstrom M, Visintin I, et al. Molecular phenotyping of human ovarian cancer stem cells unravels the mechanisms for repair and chemoresistance. *Cell Cycle*. 2009;8:158-166. doi: 10.4161/cc.8.1.7533
62. Szajnik M, Szczepanski MJ, Czystowska M, Elishaev E, Mandapathil M, Nowak-Markwitz E, Spaczynski M, Whiteside TL. TLR4 signaling induced by lipopolysaccharide or paclitaxel regulates tumor survival and chemoresistance in ovarian cancer. *Oncogene*. 2009;28:4353-4363. doi: 10.1038/onc.2009.289

63. Nguyen VHL, Hough R, Bernaudo S, Peng C. Wnt/beta-catenin signalling in ovarian cancer: Insights into its hyperactivation and function in tumorigenesis. *J Ovarian Res*. 2019;12:122. doi: 10.1186/s13048-019-0596-z
64. O'Brien K, Ughetto S, Mahjoum S, Nair AV, Breakefield XO. Uptake, functionality, and re-release of extracellular vesicle-encapsulated cargo. *Cell Rep*. 2022;39:110651. doi: 10.1016/j.celrep.2022.110651
65. Fang T, Lv H, Lv G, Li T, Wang C, Han Q, Yu L, Su B, Guo L, Huang S, et al. Tumor-derived exosomal miR-1247-3p induces cancer-associated fibroblast activation to foster lung metastasis of liver cancer. *Nat Commun*. 2018;9:191. doi: 10.1038/s41467-017-02583-0
66. Becker A, Thakur BK, Weiss JM, Kim HS, Peinado H, Lyden D. Extracellular Vesicles in Cancer: Cell-to-Cell Mediators of Metastasis. *Cancer Cell*. 2016;30:836-848. doi: 10.1016/j.ccell.2016.10.009
67. Keklikoglou I, Cianciaruso C, Guc E, Squadrito ML, Spring LM, Tazzyman S, Lambein L, Poissonnier A, Ferraro GB, Baer C, et al. Chemotherapy elicits pro-metastatic extracellular vesicles in breast cancer models. *Nat Cell Biol*. 2019;21:190-202. doi: 10.1038/s41556-018-0256-3
68. Nazimek K, Bustos-Moran E, Blas-Rus N, Nowak B, Toton-Zuranska J, Seweryn MT, Wolkow P, Woznicka O, Szatanek R, Siedlar M, et al. Antibodies Enhance the Suppressive Activity of Extracellular Vesicles in Mouse Delayed-Type Hypersensitivity. *Pharmaceuticals (Basel)*. 2021;14. doi: 10.3390/ph14080734
69. Nazimek K, Ptak W, Nowak B, Ptak M, Askenase PW, Bryniarski K. Macrophages play an essential role in antigen-specific immune suppression mediated by T CD8(+) cell-derived exosomes. *Immunology*. 2015;146:23-32. doi: 10.1111/imm.12466
70. Askenase PW. Extracellular Vesicle (EV) Targeted Cells Release Secondary Effector EVs: Indication of How To Account for Histocompatibility and Disease Specificity of EV Treatments. *J Extracell Vesicles*. 2025;14:e70076. doi: 10.1002/jev2.70076
71. Cooper J, Giancotti FG. Integrin Signaling in Cancer: Mechanotransduction, Stemness, Epithelial Plasticity, and Therapeutic Resistance. *Cancer Cell*. 2019;35:347-367. doi: 10.1016/j.ccell.2019.01.007
72. Kessenbrock K, Wang CY, Werb Z. Matrix metalloproteinases in stem cell regulation and cancer. *Matrix Biol*. 2015;44-46:184-190. doi: 10.1016/j.matbio.2015.01.022
73. Chen K, Xu M, Lu F, He Y. Development of Matrix Metalloproteinases-Mediated Extracellular Matrix Remodeling in Regenerative Medicine: A Mini Review. *Tissue Eng Regen Med*. 2023;20:661-670. doi: 10.1007/s13770-023-00536-x
74. Fukasawa M, Varlamov O, Eng WS, Sollner TH, Rothman JE. Localization and activity of the SNARE Ykt6 determined by its regulatory domain and palmitoylation. *Proc Natl Acad Sci U S A*. 2004;101:4815-4820. doi: 10.1073/pnas.0401183101
75. Kriegenburg F, Bas L, Gao J, Ungermann C, Kraft C. The multi-functional SNARE protein Ykt6 in autophagosomal fusion processes. *Cell Cycle*. 2019;18:639-651. doi: 10.1080/15384101.2019.1580488
76. Lee SB, Park YS, Sung JS, Lee JW, Kim B, Kim YH. Tumor Suppressor miR-584-5p Inhibits Migration and Invasion in Smoking Related Non-Small Cell Lung Cancer Cells by Targeting YKT6. *Cancers (Basel)*. 2021;13. doi: 10.3390/cancers13051159
77. Zhang X, ML GD, Zhang X, Chen Y. A pan-cancer analysis of the oncogenic role of YKT6 in human tumors. *Medicine (Baltimore)*. 2023;102:e33546. doi: 10.1097/MD.0000000000033546
78. Zhang L, Wang S, Wang L. Comprehensive analysis identifies YKT6 as a potential prognostic and diagnostic biomarker in lung adenocarcinoma. *BMC Cancer*. 2024;24:1235. doi: 10.1186/s12885-024-12975-3

79. Gross JC, Chaudhary V, Bartscherer K, Boutros M. Active Wnt proteins are secreted on exosomes. *Nat Cell Biol*. 2012;14:1036-1045. doi: 10.1038/ncb2574
80. Ruiz-Martinez M, Navarro A, Marrades RM, Vinolas N, Santasusagna S, Munoz C, Ramirez J, Molins L, Monzo M. YKT6 expression, exosome release, and survival in non-small cell lung cancer. *Oncotarget*. 2016;7:51515-51524. doi: 10.18632/oncotarget.9862
81. Linnemannstons K, Witte L, Karuna MP, Kittel JC, Danieli A, Muller D, Nitsch L, Honemann-Capito M, Grawe F, Wodarz A, et al. Ykt6-dependent endosomal recycling is required for Wnt secretion in the Drosophila wing epithelium. *Development*. 2020;147. doi: 10.1242/dev.185421
82. Sun C, Wang P, Dong W, Liu H, Sun J, Zhao L. LncRNA PVT1 promotes exosome secretion through YKT6, RAB7, and VAMP3 in pancreatic cancer. *Aging (Albany NY)*. 2020;12:10427-10440. doi: 10.18632/aging.103268
83. Vidal F, Guerby P, Luyckx M, Haddad P, Stoeckle E, Morice P, Leblanc E, Lecuru F, Darai E, Classe JM, et al. Are Early Relapses in Advanced-Stage Ovarian Cancer Doomed to a Poor Prognosis? *PLoS One*. 2016;11:e0147787. doi: 10.1371/journal.pone.0147787
84. Soyama H, Takano M, Miyamoto M, Yoshikawa T, Aoyama T, Goto T, Hirata J, Suzuki A, Sasa H, Furuya K. Factors favouring long-term survival following recurrence in ovarian cancer. *Molecular and clinical oncology*. 2017;7:42-46. doi: 10.3892/mco.2017.1266
85. Tudrej P, Kujawa KA, Cortez AJ, Lisowska KM. Characteristics of in Vivo Model Systems for Ovarian Cancer Studies. *Diagnostics (Basel)*. 2019;9. doi: 10.3390/diagnostics9030120
86. Barker KT, Yogev O. Establishment of In Vivo Acquired Resistance to Chemotherapy Via Individual Dose Escalation Treatment Regime. *Methods Mol Biol*. 2022;2535:73-83. doi: 10.1007/978-1-0716-2513-2_6
87. Bahar E, Kim JY, Kim HS, Yoon H. Establishment of Acquired Cisplatin Resistance in Ovarian Cancer Cell Lines Characterized by Enriched Metastatic Properties with Increased Twist Expression. *Int J Mol Sci*. 2020;21. doi: 10.3390/ijms21207613
88. Fox A, Leonard GD, Adzibolosu N, Wong T, Tedja R, Sharma S, Gogoi R, Morris R, Mor G, Fehl C, et al. Adipose microenvironment promotes hypersialylation of ovarian cancer cells. *Front Oncol*. 2024;14:1432333. doi: 10.3389/fonc.2024.1432333
89. Tedja R, Alvero AB, Fox A, Cardenas C, Pitruzzello M, Chehade H, Bawa T, Adzibolosu N, Gogoi R, Mor G. Generation of Stable Epithelial-Mesenchymal Hybrid Cancer Cells with Tumorigenic Potential. *Cancers (Basel)*. 2023;15. doi: 10.3390/cancers15030684
90. McCloskey CW, Goldberg RL, Carter LE, Gamwell LF, Al-Hujaily EM, Collins O, Macdonald EA, Garson K, Daneshmand M, Carmona E, et al. A new spontaneously transformed syngeneic model of high-grade serous ovarian cancer with a tumor-initiating cell population. *Front Oncol*. 2014;4:53. doi: 10.3389/fonc.2014.00053
91. Simpson CR, Kelly HM, Murphy CM. Synergistic use of biomaterials and licensed therapeutics to manipulate bone remodelling and promote non-union fracture repair. *Adv Drug Deliv Rev*. 2020;160:212-233. doi: 10.1016/j.addr.2020.10.011
92. Cheng W, Xu C, Su Y, Shen Y, Yang Q, Zhao Y, Zhao Y, Liu Y. Engineered Extracellular Vesicles: A potential treatment for regeneration. *iScience*. 2023;26:108282. doi: 10.1016/j.isci.2023.108282
93. Zhao S, Di Y, Fan H, Xu C, Li H, Wang Y, Wang W, Li C, Wang J. Targeted delivery of extracellular vesicles: the mechanisms, techniques and therapeutic applications. *Mol Biomed*. 2024;5:60. doi: 10.1186/s43556-024-00230-x
94. Frolova L, Li ITS. Targeting Capabilities of Native and Bioengineered Extracellular Vesicles for Drug Delivery. *Bioengineering (Basel)*. 2022;9. doi: 10.3390/bioengineering9100496
95. Stranford DM, Simons LM, Berman KE, Cheng L, DiBiase BN, Hung ME, Lucks JB, Hultquist JF, Leonard JN. Genetically encoding multiple functionalities into extracellular vesicles for the

targeted delivery of biologics to T cells. *Nat Biomed Eng*. 2024;8:397-414. doi: 10.1038/s41551-023-01142-x
96. Ng CY, Kee LT, Al-Masawa ME, Lee QH, Subramaniam T, Kok D, Ng MH, Law JX. Scalable Production of Extracellular Vesicles and Its Therapeutic Values: A Review. *Int J Mol Sci*. 2022;23. doi: 10.3390/ijms23147986
97. Kim HK, Choi Y, Kim KH, Byun Y, Kim TH, Kim JH, An SH, Bae D, Choi MK, Lee M, et al. Scalable production of siRNA-encapsulated extracellular vesicles for the inhibition of KRAS-mutant cancer using acoustic shock waves. *J Extracell Vesicles*. 2024;13:e12508. doi: 10.1002/jev2.12508
98. Li J, Jiang K, Qiu X, Li M, Hao Q, Wei L, Zhang W, Chen B, Xin X. Overexpression of CXCR4 is significantly associated with cisplatin-based chemotherapy resistance and can be a prognostic factor in epithelial ovarian cancer. *BMB Rep*. 2014;47:33-38. doi: 10.5483/bmbrep.2014.47.1.069
99. Matsui T, Jiang P, Nakano S, Sakamaki Y, Yamamoto H, Mizushima N. Autophagosomal YKT6 is required for fusion with lysosomes independently of syntaxin 17. *J Cell Biol*. 2018;217:2633-2645. doi: 10.1083/jcb.201712058
100. Stewart SA, Dykxhoorn DM, Palliser D, Mizuno H, Yu EY, An DS, Sabatini DM, Chen IS, Hahn WC, Sharp PA, et al. Lentivirus-delivered stable gene silencing by RNAi in primary cells. *RNA*. 2003;9:493-501. doi: 10.1261/rna.2192803
101. Wang L, Lu X, Chopp M, Li C, Zhang Y, Szalad A, Liu XS, Zhang ZG. Comparative proteomic analysis of exosomes derived from endothelial cells and Schwann cells. *PLoS One*. 2023;18:e0290155. doi: 10.1371/journal.pone.0290155
102. Li C, Zhang Y, Levin AM, Fan BY, Teng H, Ghannam MM, Chopp M, Zhang ZG. Distal Axonal Proteins and Their Related MiRNAs in Cultured Cortical Neurons. *Mol Neurobiol*. 2019;56:2703-2713. doi: 10.1007/s12035-018-1266-7
103. Chen EY, Tan CM, Kou Y, Duan Q, Wang Z, Meirelles GV, Clark NR, Ma'ayan A. Enrichr: interactive and collaborative HTML5 gene list enrichment analysis tool. *BMC Bioinformatics*. 2013;14:128. doi: 10.1186/1471-2105-14-128
104. Alvero AB, Montagna MK, Chen R, Kim KH, Kyungjin K, Visintin I, Fu HH, Brown D, Mor G. NV-128, a novel isoflavone derivative, induces caspase-independent cell death through the Akt/mammalian target of rapamycin pathway. *Cancer*. 2009;115:3204-3216. doi: 10.1002/cncr.24397
105. Kluger HM, McCarthy MM, Alvero AB, Sznol M, Ariyan S, Camp RL, Rimm DL, Mor G. The X-linked inhibitor of apoptosis protein (XIAP) is up-regulated in metastatic melanoma, and XIAP cleavage by Phenoxodiol is associated with Carboplatin sensitization. *J Transl Med*. 2007;5:6. doi: 10.1186/1479-5876-5-6
106. Caldwell C, Rottman JB, Paces W, Bueche E, Reitsma S, Gibb J, Adisetiyo V, Haas MS, Heath H, Newman W, et al. Validation of a DKK1 RNAscope chromogenic in situ hybridization assay for gastric and gastroesophageal junction adenocarcinoma tumors. *Sci Rep*. 2021;11:9920. doi: 10.1038/s41598-021-89060-3
107. Ball JB, McNulty CJ, Green-Fulgham SM, Dragavon JM, Correia Rocha IR, Finch MR, Prevost ED, Siddique, II, Woodall BJ, Watkins LR, et al. Combining RNAscope and immunohistochemistry to visualize inflammatory gene products in neurons and microglia. *Front Mol Neurosci*. 2023;16:1225847. doi: 10.3389/fnmol.2023.1225847
108. Zhang Y, Qin Y, Chopp M, Li C, Kemper A, Liu X, Wang X, Zhang L, Zhang ZG. Ischemic Cerebral Endothelial Cell-Derived Exosomes Promote Axonal Growth. *Stroke*. 2020;51:3701-3712. doi: 10.1161/STROKEAHA.120.031728

109. Zhang Y, Ueno Y, Liu XS, Buller B, Wang X, Chopp M, Zhang ZG. The MicroRNA-17-92 cluster enhances axonal outgrowth in embryonic cortical neurons. *J Neurosci*. 2013;33:6885-6894. doi: 10.1523/JNEUROSCI.5180-12.2013
110. Mittal S, Kumar S, Gupta P, Singh M, Chaluvally-Raghavan P, Pradeep S. Protocol for the isolation of tumor cell-derived extracellular vesicles followed by in vivo metastasis assessment in a murine ovarian cancer model. *STAR Protoc*. 2024;5:102943. doi: 10.1016/j.xpro.2024.102943
111. Wang X, Chen J, Li Z, Huang D, Yi X, Wu J, Zhong T. An Enrichment Method for Small Extracellular Vesicles Derived from Liver Cancer Tissue. *J Vis Exp*. 2023. doi: 10.3791/64499